9.03 Formation of Earth's Core

D. C. Rubie, Universität Bayreuth, Bayreuth, Germany

F. Nimmo, University of California, Santa Cruz, CA, USA

H. J. Melosh, University of Arizona, Tucson, AZ, USA

9.03.1 Core Formation in the Earth and Terrestrial Planets

9.03.1.1 Introduction and Present State of Cores in Solar System Bodies

The Earth's metallic core, comprising 32% of the total mass of the planet, lies beneath a silicate mantle, with the core–mantle boundary (CMB) located at a depth of 2891 km. The differentiation of the Earth into a metallic core and silicate mantle occurred during the accretion of the planet and represents the most important differentiation event in its history. Other terrestrial planets (e.g., Mercury, Venus, and Mars) and small asteroid bodies also underwent such differentiation events during the early history of the solar system and are thus important for providing additional information that helps in understanding differentiation of the Earth.

'Core formation' implies a single event, whereas in reality the core of the Earth most likely formed through a long series of events, over an extended time period. In this chapter, we consider the period up to which the core reached roughly 99% of its present-day mass; its later evolution is considered (Chapter 9.09). Other relevant chapters in this volume are concerned with the early Earth's composition (Chapter 9.02) and the terrestrial magma ocean (Chapter 9.04).

Here we first provide a general outline of the physical processes that are likely to be involved in core formation, including a discussion of the various uncertainties that arise. The second part of this chapter is focused on observations and experimental data

that place constraints on the processes that operated and the state of the core during its formation.

The ultimate reason that the Earth and planets have cores is a matter of elementary physics: because metallic iron and its alloys are denser than silicates or ices, the most stable arrangement of a rotating, self-gravitating mass of material is an oblate spheroid with the dense iron at the center. Although the physical imperative driving core formation is simple, its realization is complicated by the usual factors of contingency and history. How the cores of the terrestrial planets came to their present configuration depends on what materials were available to make them, at what time and in what condition this material was added, and then how this mass of material evolved with time.

The origin and abundance of the elements of our solar system is now understood as the consequence of (mainly) stellar nucleosynthesis. Nuclear burning in stars created the elements and established their abundances in our solar system. Iron, as the end product of nuclear burning, owes its large abundance to its maximal nuclear stability. However, this review cannot go that far back. Fortunately, there are many good reviews of current ideas about the origin of the elements in our solar system (e.g., Busso *et al.*, 1999; Turan, 1984). But we cannot entirely ignore this aspect of solar system history, because one of the major developments in the past few years follows from the contingent circumstance that the solar system formed in conjunction with one or more nearby supernovas. These catastrophic events produced a substantial abundance of the short-lived radioactive isotopes ^{60}Fe and ^{26}Al, among many others. The consequences of this accident reverberate through our present solar system in ways that are just now becoming clear.

However, before exploring the antecedents of planetary cores in detail, we first consider what is known. All of the terrestrial planets and satellites, except perhaps Earth's moon, are believed to possess a dense, probably metallic, core. This belief is founded mainly on the density and moment of inertia of each body. If the average (uncompressed) density of a planet is much larger than the density of the material at its surface, one must infer that its interior is more dense. A homogeneous body has a moment of inertia ratio C/MR^2 equal to 0.400. Substantially smaller values of this ratio indicate a central mass concentration, one that usually implies a change of state or composition in the interior (we here exclude the slight decrease in this ratio due to self compression).

The size of Earth's core is known accurately from seismic data. The limited operating lifetime of the Apollo lunar seismic array provided only ambiguous evidence for a lunar core, and no seismic data exist for any other solar system object. Mercury presently possesses a small magnetic field and Mars probably had one in the past, suggesting the presence of metallic, fluid, and electrically conducting cores in these planets. Although Venus and Mars do not have magnetic fields at the present time, spacecraft measurements of their k_2 Love number indicate a large deformation in response to solar tides, implying an at least partially liquid core; observations of lunar nutations likewise suggest a liquid lunar core. **Table 1** summarizes our present knowledge of cores in the terrestrial planets and other bodies in the solar system.

9.03.1.2 The Relevance of Iron Meteorites

During the two centuries after meteorites were first accepted as samples of other bodies in our solar system, approximately 18 000 iron meteorites have been cataloged that, on the basis of trace element groupings, appear to have originated as the cores of approximately 100 separate bodies. These iron-meteorite parent bodies were small: cooling rates estimated from Fe/Ni diffusion profiles across taenite/kamacite crystal contacts suggest parent body diameters ranging from 30 to 100 km (Wasson, 1985: Chabot and Haack, 2006). Until recently, it was believed that the iron-meteorite parent bodies differentiated into an iron–nickel core and mantle sometime after most of the other meteorites, principally chondrites, had formed. However, recent dates using the extinct (9 My half-life) ^{182}Hf–^{182}W radioactive system have demonstrated that magmatic iron meteorites actually formed about 3 My before most chondrites (Scherstén *et al.*, 2006). This is nearly the same age as the heretofore oldest objects in the solar system, the calcium–aluminum inclusions (CAI) found in carbonaceous chondrites. This observation has completely changed our perception of the events in the early solar system and, in particular, the nature of the planetesimals that accumulated to form the Earth and other terrestrial planets. Previous to this revision in the age of the iron meteorites, the source of the heat necessary to differentiate the iron-meteorite parent bodies was obscure: suggestions ran the gamut from electromagnetic induction in solar flares to lightening in the solar nebula. Although the short-lived radioactivities ^{26}Al (half-life 0.74 My) and ^{60}Fe (1.5 My) were known to

Table 1 Planetary and satellite cores

Body	Mean density (Mg m^{-3})	Moment of inertia factor C/MR^2	Love number k_2	Mean planet radius, R_p (km)	Core radius (km)	Magnetic moment T R_p^3	Core mechanical state	Composition
Mercury	5.427	0.33	?	2440	~1600	4×10^{-7} [a]	Liquid?	Fe, Ni, ?
Venus	5.204	0.33	~0.25	6051.8	~3200	None at present	Liquid	Fe, Ni, ?
Earth	5.515	0.3308	0.299	6371.0	3485	6.1×10^{-5}	Liquid outer, solid inner core	Fe, Ni, FeO/FeS ?
Moon	3.344	0.3935	0.0302	1737.53	400?	None at present	Liquid?	Fe, Ni, ?
Mars	3.933	0.366	~0.14	3389.9	~1700	Only local sources	Liquid?	Fe, Ni, FeO/FeS ?
Io[b]	3.53	0.378	?	1821	~950	None	Liquid?	Fe, Ni, FeS ?
Europa[b]	2.99	0.346	?	1565	200–700	None	Liquid?	Fe, Ni FeS ?
Ganymede[b]	1.94	0.312	?	2631	650–900	7.15×10^{-7} [b]	Liquid?	Fe,Ni, FeS ?
Callisto	1.83	0.355	?	2410	None?	None	—	—

[a] Russell and Luhmann (1997).
[b] Schubert *et al.* (2004).
Unless otherwise noted, data are from Yoder (1995).
'?' indicates that values are currently unknown.

have been present in the early solar system, it was believed that by the time that the iron-meteorite parent bodies formed these potential heat sources had burned themselves out. However, with the new ages, a new view emerges.

The effectiveness of the heating caused by the decay of a radioactive isotope of a stable element can be gauged from the following formula that gives the maximum temperature rise ΔT occurring in a completely insulated sample of material during the time subsequent to its isolation:

$$\Delta T = \frac{f \; C_{\mathrm{m}} \; E_{\mathrm{D}}}{c_p} \qquad [1]$$

where c_p is the heat capacity of the material, C_{m} is the concentration of the stable element in the material, f is the fraction of radioactive isotope at the beginning of the isolation interval, and E_{D} is the nuclear decay energy released into heat (we do not count the energy of neutrinos emitted during beta decay). **Table 2** lists the values of this temperature rise for undifferentiated material of carbonaceous chondrite composition at the time of CAI and iron-meteorite formation, and at the time that the bulk of the chondrites formed, 3 million years later.

The principal implication of this recent finding for core formation in the Earth is that many (if not most) of the planetesimals that accumulated to form the major planets possessed metallic cores at the time of their accretion. As yet, the consequences of accretional impacts among partially molten planetesimals are not well studied. However, it is clear that if the planetesimals contributing to the growth of planetary embryos had already formed iron cores, chemical equilibration between iron and silicates initially occurred in a low-pressure regime. In addition, the iron that was added to the growing embryos might not have been in the form of small, dispersed droplets.

Just how the iron core of an impacting planetesimal mixes with the existing surface is presently somewhat unclear. Even the largest meteorite impacts on the present Earth seldom preserve more than a trace of the projectile. In most cases the projectile, if it can be identified at all, is only revealed by geochemical or isotopic tracers in the rock melted by the impact. The largest intact remnant of an impactor presently known is a 25-cm-diameter fragment of LL6 chondrite discovered in the melt sheet of the *c.* 70-km-diameter Morokweng crater (Maier *et al.*, 2006). The impactor that created the 170-km-diameter Chicxulub crater is known only from a few millimeter-size fragments recovered from a deep-sea core (Kyte, 1998). The projectiles that created these craters are at the low end of the size spectrum we

Table 2 Temperature rise of undifferentiated carbonaceous chondrites due to radioactive decay

Radioisotope	Half-life (My)	Fractional abundance of isotope at CAI time, f	Nuclear decay energy, E_D (J kg^{-1})	ΔT at CAI time (K)	ΔT 3 My later (K)
^{26}Al	0.74	$(5–7) \times 10^{-5}$	1.16×10^{13}[a]	4170	251
^{60}Fe	1.5	4.4×10^{-6}[b]	4.43×10^{12}	2960	740

[a]Schramm *et al.* (1970).
[b]Quitté *et al.* (2005).
Assuming the solar system abundances of Anders and Gervesse (1989) and heat capacity $c_p = 1200\,\mathrm{J\,kg^{-1}\,K}$. Abundances of Fe and Al are assumed to be chondritic, at 18.2 wt.% and 0.865 wt.%, respectively (Lodders and Fegley, 1998).

expect for planetesimals: the diameter of the Morokweng impactor was about 4 km or more, while the Chicxulub impactor was probably about 15 km in diameter. Both objects probably impacted near the average velocity for asteroidal impactors on the Earth, about 17 km s^{-1}. Although this velocity is substantially higher than the encounter velocity of the nearly formed Earth with infalling planetesimals (less than about 10 km s^{-1}, or a factor of more than three times less energy than current asteroidal impacts), it still illustrates the fact that impacts typically disrupt the impactor and whatever the arrangement of materials might have been in the impacting objects; this arrangement is greatly distorted during the impact event.

If we can extrapolate from these observations to the impacts of much larger objects, one would conclude that it makes little difference whether the impacting planetesimal was differentiated or not – in either case the result of the impact is a finely dispersed mixture of melted target and projectile material. On the other hand, computer simulations of the much larger moon-forming impact show that the core of a planet-size impactor remains mostly together in a discrete mass during the impact and appears to merge almost *en masse* with the Earth's core (Canup, 2004). In these simulations, however, each 'particle' representing the material of the Earth and projectile is about 200 km in diameter, so that it is not possible to resolve details of how the iron mass from the projectile core really interacts with the Earth's mantle and core. It thus seems possible that the cores of large planetesimals might remain together in homogeneous masses too large for chemical equilibration (i.e., larger than a few centimeters) with their surroundings, at least at the beginning of their descent into the Earth's mantle. This is an area needing further study from the impact perspective. Later in this review we discuss the probable fate of such large masses of iron in their inexorable fall toward the Earth's core.

9.03.1.3 History of Ideas on Core Formation

Ideas on how the Earth's core formed have shifted dramatically over the past century. At the beginning of the twentieth century most geophysicists believed, following Lord Kelvin, that the Earth began in a completely molten state and its subsequent history was one of secular cooling and solidification (Thomson and Tait, 1883, p. 482). As late as 1952, Harold Jeffreys found core formation totally unproblematic, because dense iron would inevitably sink through the liquid proto-mantle (Jeffreys, 1952, p. 271). However, about the same time, Urey (1952) was elaborating Chamberlin's (1916) hypothesis that the planets had formed from a swarm of small, cold, mutually gravitating 'planetesimals'. In Urey's analysis, core formation becomes highly problematic. The apparent difficulty posed by Urey's view initiated much of our current thinking about how the Earth's metallic iron core originated.

In his famous book *The Planets*, Urey (1952) presented a model of planet formation that strongly appealed to physicists, although, as we shall soon see, it lacked many aspects of reality. Urey approximated the growing Earth as a spherical, homogeneous, isotropic body of radius r that grew from cold matter in space by the addition of infinitesimally thin shells of thickness dr. In this model he equated the gravitational energy of infalling matter, $-GM(r)/r$ per unit mass, where G is Newton's gravitational constant and $M(r)$ is the mass of the nascent Earth at radius r, with the heat gained after the matter accreted to the Earth. This energy was apportioned between heating of the added mass, heat conduction into the interior, and thermal radiation to space. Because the shell of added matter is very thin, thermal radiation dominates and the planet accretes at very low temperatures.

Models of this kind led Hanks and Anderson (1969) to discover that even if the Earth accreted in as little as 1 My it would not reach the melting temperature of

rock anywhere in its interior. They showed that radioactive heating would only warm the Earth's interior to the melting point much later, initiating core formation as late as 1.6 Gy after its formation.

By the 1970s, however, study of lead isotopes in ancient crustal rocks indicated that the core had formed within a few hundred million years of the iron meteorites (Gancarz and Wasserburg, 1977), and that a problem existed with the models for thermal evolution of the Earth. Safronov (1978) and Kaula (1979) independently suggested that Urey's model, in which thin shells of infalling matter radiated most of its energy to space, is too drastic. If the impacting planetesimals were of moderate size, a few kilometers or more in diameter, some substantial, but not easily computed, fraction h of the gravitational energy would be buried in the planet. Although this solution has seemed attractive for many decades, it has one central flaw: because the gravitational energy of the planet is initially rather small, the energy added by each unit of mass, $hG\,M(r)/r$, increases roughly as the square of the radius of the Earth. The center of the Earth thus starts out cold, although a hotter, molten, outer shell eventually develops around it. We thus end up with an Earth that is thermally inside-out: cold in the center, hot on the outside.

This apparent conundrum over the initial thermal structure of the Earth led to a series of clever examinations of the stability of a shell of molten, segregated iron in the hot outer portion of the Earth. Elsasser (1963) suggested that a shell of molten iron would push its way to the Earth's center by diapiric instabilities. Later, Stevenson (1981) showed that this instability is even stronger than Elsasser suspected, and that the iron would actually fracture the cold kernel of the Earth on a timescale of hours, supposing that such a global iron layer ever had time to form.

In our modern era, in which a much more catastrophic view of Earth's formation reigns (Wetherill, 1985), the problematic initial thermal profile of the Earth is ameliorated by the ability of gigantic impacts to implant heat deep into a growing planet (Melosh, 1990). Deep, strong heating and core formation can be initiated by impacts themselves, given only that they are large and late enough (Tonks and Melosh, 1992). Magma oceans are now seen as an inevitable consequence of the late accretion of planet-scale protoplanets (Tonks and Melosh, 1993). In this era the problem is not so much how cores form, as to how, and under what circumstances, iron and silicate may have equilibrated chemically, and how the current inventories of chemical elements in the crusts and mantles of the Earth and planets were established.

9.03.2 Physics of Core Formation

The Earth is the end product of multiple collisions between smaller protoplanets. This process of accretion results in increased temperatures and, ultimately, melting on a planetary scale. As discussed below, differentiation is unavoidable once melting begins; thus, the accretion process is intimately connected to the manner in which the Earth, and its precursor bodies, underwent differentiation and core formation. In this section, our theoretical understanding of the accretion process and its consequences for core formation are discussed; in Section 9.03.3, observational and experimental constraints on these processes are outlined.

Earlier reviews and discussions of the processes enumerated here may be found in Stevenson (1989, 1990), Rubie *et al.* (2003), Walter and Trønnes (2004), and Wood *et al.* (2006). The collection of papers edited by Canup and Righter (2000) is also highly recommended.

9.03.2.1 Accretion

The basic physics of planetary accretion are now reasonably well understood, although many details remain obscure (see Wetherill (1990) and Chambers (2003) for useful reviews). Growth of kilometer-sized objects (planetesimals) from the initial dusty, gaseous nebula must have been a rapid process (occurring within approximately 10^3 years), because otherwise the dust grains would have been lost due to gas drag. At sizes >1 km, mutual gravitational interactions between planetesimals become important. Furthermore, because the largest bodies experience the greatest gravitational focusing, they tend to grow at the expense of smaller surrounding objects. This 'runaway growth' phase, if uninterrupted, can potentially result in the development of tens to hundreds of Mars- to Moon-sized embryos in $\sim 10^5$ years at a distance of around 1 astronomical unit (AU) from the Sun (Wetherill and Stewart, 1993). However, runaway growth slows down as the initial swarm of small bodies becomes exhausted and the velocity dispersion of the remaining larger bodies increases (Kokubo and Ida, 1998). Thus, the development of Moon- to Mars-sized embryos probably took $\sim 10^6$ years at 1 AU (Weidenschilling *et al.*, 1997), and

involved collisions both between comparably sized embryos, and between embryos and smaller, left-over planetesimals. Based on astronomical observations of dust disks (Haisch *et al.*, 2001), the dissipation of any remaining nebular gas also takes place after a few million years; the dissipation timescale of gas has implications both for the orbital evolution of the bodies (e.g., Kominami *et al.*, 2005), their volatile inventories (e.g., Porcelli *et al.*, 2001), and their surface temperatures (e.g., Abe, 1997), and is currently a critical unknown parameter. Noble gas isotopes, in particular those of xenon, have been used to argue for a primordial, dense, radiatively opaque terrestrial atmosphere (e.g., Porcelli *et al.*, 2001, Halliday, 2003), but this interpretation remains controversial (*see* Chapter 9.02).

Collisional growth processes lead to a peculiar size–frequency spectrum of the accumulating bodies. At first, the runaway accretional processes produce a spectrum in which the cumulative number of objects (the number of objects equal to, or greater, than diameter D) is proportional to an inverse power of their diameter, generally of form $N_{\mathrm{cum}}(D) \sim D^{-b}$, where b is often approximately 2 (Melosh, 1990). One of the principal characteristics of such a distribution is that although the smallest bodies overwhelmingly dominate in number, most of the mass and energy resides in the very largest objects. Accretional impacts are thus catastrophic in the sense that objects at the largest end of the size spectrum dominate planetary growth. Later, during oligarchic growth at the planetary embryo scale, the large bodies represent an even larger fraction of the size spectrum and giant impacts, that is, impacts between bodies of comparable size dominate planetary growth history.

The subsequent growth of Earth-sized bodies from smaller Mars-sized embyros is slow, because the embryos grow only when mutual gravitational perturbations lead to crossing orbits. Numerical simulations show that Earth-sized bodies take 10–100 My to develop (e.g., Chambers and Wetherill, 1998; Agnor *et al.*, 1999; Morbidelli *et al.*, 2000; Raymond *et al.*, 2004), and do so through a relatively small number of collisions between objects of roughly comparable sizes. A recent result of great importance is that geochemical observations, notably using the hafnium–tungsten (Hf–W) isotopic system, have been used to verify the timescales obtained theoretically through computer simulations of accretion processes (see Section 9.03.3.1).

It should be noted that an important implicit assumption of most late-stage accretion models is that collisions result in mergers. In fact, this assumption is unlikely to be correct (Agnor and Asphaug, 2004; Asphaug *et al.*, 2006) and many collisions may involve little net transfer of material, though both transient heating and transfer of angular momentum will occur. In fact nearly 80% of the mantle of Mercury may have been 'lost' by collisional erosion after core formation, thus explaining the huge size of its metallic core (Benz *et al.*, 1988). Such disruptive collisions may also have influenced the evolution of the Earth and could explain an excess of Fe in the Earth's bulk composition relative to C1 chondrites (Palme *et al.*, 2003).

Figure 1(a) shows a schematic example (obtained by splicing together two different accretion simulations) of how a roughly Earth-mass ($1 M_{\mathrm{e}}$) body might grow. Here the initial mass distribution consists of 11 lunar-mass embryos ($\approx 0.01 M_{\mathrm{e}}$) and 900 smaller ($\approx 0.001 M_{\mathrm{e}}$) noninteracting planetesimals centered around 1 AU. The solid line shows the increase in mass, and the crosses show the impactor:target mass ratio γ (both in log units). The early stage of growth is characterized by steady collision with small planetesimals, and occasional collisions with other, comparably sized embryos (e.g., at 0.068 and 1.9 My). Because the planetesimals do not grow, the impactor:target mass ratio γ of colliding planetesimals declines with time; embryo–embryo collisions show up clearly, having $\gamma \sim 1$. At 2 My, the growing object has a mass of $0.2 M_{\mathrm{e}}$ and roughly half of this mass has been delivered by large impacts. The late stage of growth consists entirely of large impacts, between embryos of comparable masses ($\gamma \sim 0.5$). This final stage takes place over a more extended timescale – in this case, the last significant collision occurs at 14 My, resulting in a final mass of $0.73 M_{\mathrm{e}}$.

One of the most important outstanding questions regarding this late-stage accretion is the amount of water that was delivered to the Earth. The presence of large quantities of water in the early mantle would have profound implications for the oxidation state and composition of the core (see Williams and Hemley (2001)); furthermore, a byproduct would be a thick steam atmosphere, which would be sufficiently insulating to ensure a magma ocean (Matsui and Abe, 1986). Although the Earth formed inside the 'snow line', where water ice becomes unstable, some of its constituent planetesimals may have been derived from greater heliocentric distances and thus contained more water. Simulations (Morbidelli *et al.*, 2000; Raymond *et al.*, 2004) suggest that a water-rich Earth is quite likely, but the stochastic nature of the outcomes

precludes a firm conclusion. Radial mixing of planetesimals is clearly not completely efficient because of the differing oxygen-isotope characteristics of Earth and Mars (e.g., Clayton and Mayeda, 1996).

9.03.2.2 Thermal Evolution

As discussed below in Section 9.03.2.3, the actual mechanisms of core formation (metal–silicate separation) that operate are dependent on the thermal state of a planetary body and at least some degree of partial melting is required. However, in addition to understanding the thermal state of the Earth during core formation, it is also important to understand the thermal histories of small bodies (planetesimals and asteroids) because these determine whether or not the material that accreted to form the Earth had already undergone core–mantle differentiation.

There are three main sources of energy that can produce the melting that is required for core formation. First, the decay of short-lived radioactive nuclides (^{26}Al and ^{60}Fe) is an important source of energy when accretion occurs very soon after the formation of the solar system (**Figure 1(b)**). (These isotopes have half-lives of 0.73×10^6 and 1.5×10^6 years, respectively.) Second, the kinetic energy delivered by impacts can be sufficient to generate local or global melting, especially during the late stages of Earth accretion (**Figures 1(b)** and **3**). Finally, as discussed below, the process of differentiation itself, by reducing the gravitational potential energy of the body, also releases heat and may lead to runaway differentiation.

9.03.2.2.1 Decay of radioactive nuclides

Thermal models show that the decay of ^{26}Al and ^{60}Fe in a body with a minimum radius of 30 km can result in maximum temperatures that range from below the Fe–FeS eutectic temperature to above silicate melting temperatures, depending on the initial concentrations of these isotopes (**Figure 2**). In contrast, the energy released through collisions between bodies less than a few hundred kilometer radius is insufficient to cause global melting (Keil *et al.*, 1997; see also Section 9.03.2.2.2). This means that the melting required for core–mantle differentiation in a small body could only occur at a very early stage during the history of the solar system – for example, within the first 1 My (Baker *et al.*, 2005). In support of the thermal models, there is geochemical evidence for large-scale melting and magma ocean formation on at least some small bodies (Greenwood *et al.*, 2005). In addition, the parent body of the HED meteorites (which is likely Asteriod-4 Vesta, 530 km in diameter) underwent early core–mantle differentiation. These considerations support the view that planetesimals that accreted to form the Earth were already differentiated (e.g., Taylor and Norman,

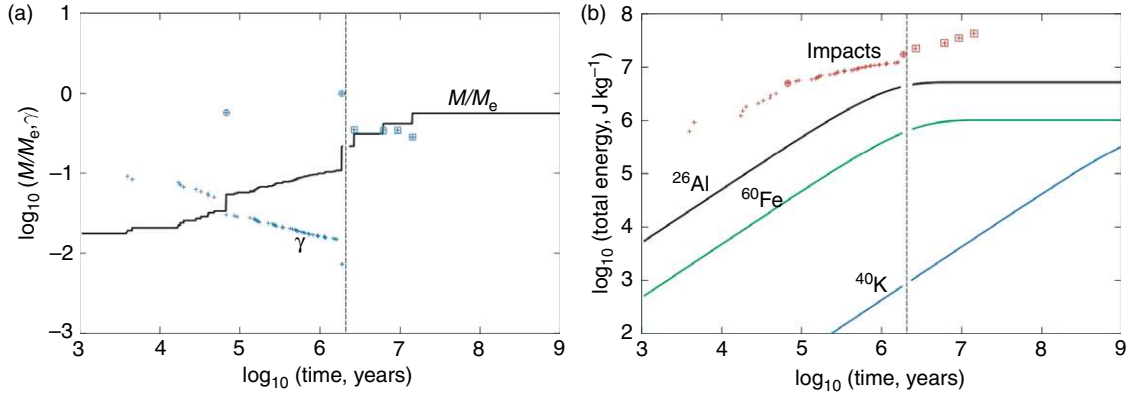

Figure 1 (a) Schematic growth of a proto-Earth, obtained by splicing two accretion simulations together. Early growth is from Agnor (unpublished) where the initial mass distribution consists of 11 embryos ($\approx 0.01 M_e$) and 900 noninteracting planetesimals ($\approx 0.001 M_e$) centred around 1 AU. Late growth is from particle 12 in run 3 of Agnor *et al.* (1999). The vertical dashed line denotes the splicing time. The solid line shows the mass evolution of the body, and the crosses denote the impactor:target mass ratio γ. Circles denote embryo–embryo collisions; squares late-stage giant impacts. The general reduction in γ prior to 2 My is a result of the fact that the planetesimals cannot merge with each other, but only with embryos. (b) Corresponding energy production (J kg^{-1}). The cumulative energy due to impacts (crosses) is calculated using eqn [2] for each impact. The solid lines show the cumulative energy associated with the decay of radioactive elements ^{26}Al, ^{60}Fe, and ^{40}K. Half-lives are 0.73 My, 1.5 My, and 1.25 Gy, respectively; initial bulk concentrations are 5×10^{-7}, 2×10^{-7}, and 4.5×10^{-7}, respectively (Ghosh and McSween, 1998; Tachibana *et al.*, 2006; Turcotte and Schubert, 2002).

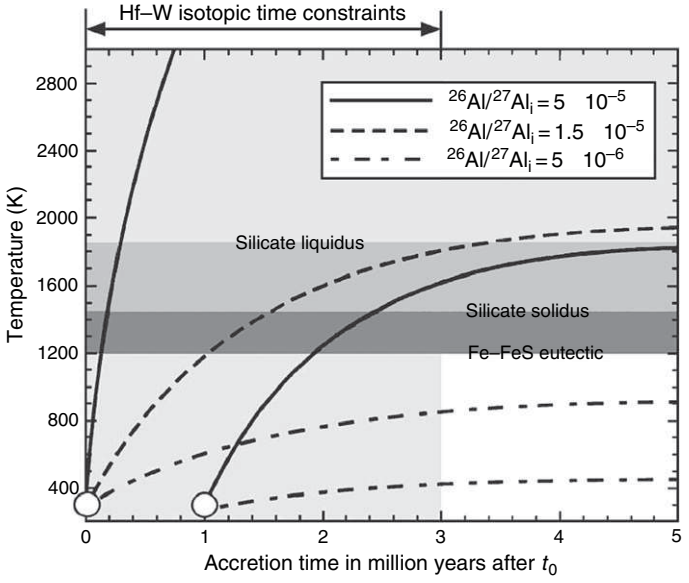

Figure 2 Models of the thermal evolution of a small body (>30 km radius) as a function of the initial concentration of ^{26}Al. Temperature is calculated as a function of time after the start of the solar system (t_0). Depending on the concentrations of ^{26}Al and ^{60}Fe and when accretion starts, maximum temperatures range from below the Fe–FeS eutectic to above the silicate liquidus (see also Yoshino *et al.*, 2003, figure 2). Reproduced from Walter MJ and Trønnes RG (2004) Early Earth differentiation. *Earth and Planetary Science Letters* 225: 253–269, with permission from Elsevier.

1990). However, if small bodies accreted somewhat later, melting and differentiation may not have occurred because the concentrations of ^{26}Al and ^{60}Fe would have been too low (**Figure 2**). The density of the solar nebula must have decreased with increasing distance from the Sun. Because the rate of a body's accretion depends on the density of the solar nebula, bodies in the outer regions would have accreted slower and therefore later, than those close to the Sun (Grimm and McSween, 1993). Thus not all planetesimals would have differentiated. Ceres is an example of an asteroid that may not have differentiated to form a metallic core (Thomas *et al.*, 2005). It is therefore currently not clear whether the Earth accreted from only differentiated bodies or a mixture of differentiated and undifferentiated bodies. The answer depends on the extent of the Earth's feeding zone during accretion.

9.03.2.2.2 Heating due to the energy of impacts

Figure 1(a) shows that the bulk of late-stage Earth accretion involves large impacts well separated in time. The energetic consequences of such impacts have been discussed elsewhere (Melosh, 1990; Benz and Cameron, 1990; Tonks and Melosh, 1993) and strongly suggest that, even in the absence of a thick primordial (insulating) atmosphere, the final stages of Earth's growth must have involved of one or more global magma oceans. This conclusion has important implications for the mode of core formation, and may be understood using the following simple analysis.

For an impact between a target of mass M and an impactor of mass γM, the mean change in energy per unit mass of the merged object due to kinetic and gravitational potential energy is

$$\Delta E = \frac{1}{1+\gamma}\left[-\frac{3}{5}\left(\frac{4\pi\rho}{3}\right)^{1/3} \times GM^{2/3}\left(1+\gamma^{5/3}-(1+\gamma)^{5/3}\right)+\frac{1}{2}\gamma V_\infty^2\right] \quad [2]$$

Here ρ is the mean density of the merged object, G is the universal gravitational constant, V_∞ is the velocity of the impactor at a large distance from the target, and the factor of $3/5$ comes from considering the binding energy of the bodies (assumed uniform) prior to and after the collision. Neglecting V_∞ and taking γ to be small, the global average temperature rise associated with one such impact is given by

$$\Delta T \approx 6000K\left(\frac{\gamma}{0.1}\right)\left(\frac{M}{M_e}\right)^{2/3} \quad [3]$$

where we have assumed that $\rho = 5000\,\mathrm{kg\,m^{-3}}$ and a heat capacity of $1\,\mathrm{kJ\,kg^{-1}\,K^{-1}}$. Note that this temperature change is a globally averaged value; for small impacts in particular, real temperatures will vary significantly with distance from the impact site.

Equation [2] is based on several simplifying assumptions. It assumes that the energy is deposited uniformly, which is unlikely to be correct. More importantly, it assumes that all the kinetic energy is converted into heat and retained. Such an assumption is unlikely to be correct for small impacts, where most of the energy is deposited at shallow depths where it can be radiated back to space (Stevenson, 1989). For larger impacts, however, the energy will be deposited at greater depths, and thus the only major energy loss mechanism is the ejection of hot material. The amount and temperature of material ejected depends strongly on the geometry of the impact, but is in general rather small compared to the target mass (Canup *et al.*, 2001). Since we are primarily concerned with large impacts ($\gamma > 0.1$), the assumption that the majority of the energy is retained as heat energy is a reasonable one. Thus, impactors with a size similar to the one that is believed to have formed the Earth's Moon (Cameron, 2000; Canup and Asphaug, 2001) probably resulted in the bulk of the Earth being melted.

Although a Mars-sized ($0.1 M_e$) proto-Earth has a smaller mass, it experiences collisions with bodies comparable in size to itself ($\gamma \approx 1$; see **Figure 1**). In this case, eqn [2] shows that $\Delta T \approx 4500\,\mathrm{K}$. Thus, it seems likely that Mars-sized embryos were also molten and thus differentiated. Although there is currently little direct evidence for an ancient Martian magma ocean (see Elkins-Tanton *et al.*, 2003), Blichert-Toft *et al.* (1999) and Borg and Draper (2003) have used Lu–Hf systematics and incompatible element abundances, respectively, to argue for such an ocean. Conversely, Righter (2003) argued that the temperatures and pressures inferred from siderophile element abundances do not necessarily require a magma ocean.

In considering the thermal effects of impacts, it may also be useful to consider the cumulative energy delivered for comparison with other sources of energy. **Figure 1(b)** shows the cumulative impact energy in $\mathrm{J\,kg^{-1}}$. The bulk of the energy is delivered by the few largest impacts, as expected. For comparison, the radioactive heat production due to one long-lived (^{40}K) and two short-lived isotopes (^{26}Al and ^{60}Fe) are shown. Long-lived isotopes have no effect at all on the thermal evolution of the Earth over its first 10 My.

The total energy associated with ^{26}Al depends very strongly on the accretion time (**Figure 2**) and in this case is roughly one order of magnitude smaller than that due to the impacts. **Figure 1(b)** shows that the thermal evolution of the Earth naturally divides into two stages: the early stage (up to ~10 My) when heating due to impacts and short-lived isotopes dominate; and the later stage, when long-lived isotopes and secular cooling are important.

Figure 3 summarizes the expected mean global temperature change due to impacts and short-lived radionuclides as a function of planetary size. The effect of a single impact (solid lines) is calculated using eqn [2] and demonstrates the strong dependence on both body mass and the impactor:target mass ratio γ. It should be re-emphasized that, particularly for small impacts, the energy will not be distributed evenly and that the calculated temperature rise is only a mean global value. The effect of ^{26}Al decay (dashed lines) does not depend on the body mass, but only on the accretion time relative to CAI formation. For small bodies, only radioactive decay contributes substantially to warming; for large

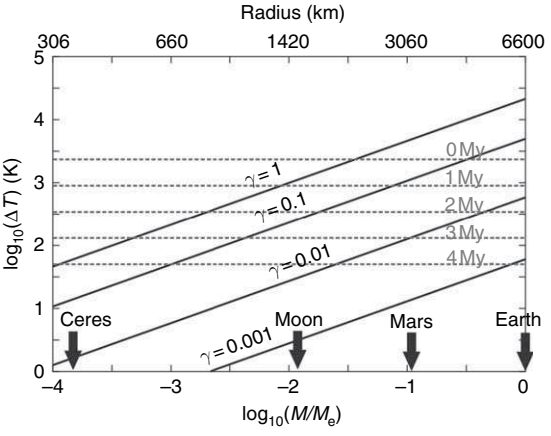

Figure 3 Mean global temperature change ΔT as a function of planetary mass (in units of M_e = one Earth mass). Solid lines show gravitational energy due to a single collision where γ denotes the impactor:target mass ratio and ΔT is calculated from eqn [2] assuming that $V_\infty = 0$, $C_p = 1000\,\mathrm{J\,kg^{-1}\,K^{-1}}$ and $\rho = 5000\,\mathrm{kg\,m^{-3}}$. Dashed lines show temperature change due to ^{26}Al decay as a function of (instantaneous) planet formation time (in million years) after solar system formation. Total energy release by ^{26}Al is $6.2 \times 10^6\,\mathrm{J\,kg^{-1}}$ (assuming 1 wt.% Al and a fractional abundance of ^{26}Al of 5×10^{-5}) and half-life is 0.73 My. Planetary melting is expected to be widespread for $\Delta T > 1000\,\mathrm{K}$. Note that heat losses by conduction or convection are neglected when calculating the temperature rise.

bodies, gravitational energy release will tend to dominate. **Figure 3** also emphasizes that the population of impactors a growing planet encounters has a very important effect on its ultimate temperature structure. If all the impactors are small ($\gamma \ll 1$) then the temperature changes are quite modest. Conversely, the later stages of planetary accretion ensure that growing bodies will encounter other bodies of similar size (i.e., $\gamma \sim 1$; Section 9.03.2.1), and thus melting is expected for bodies of roughly Moon-size and larger.

Although the average temperature jumps in large planets struck by comparable-sized objects are impressive, it must be kept in mind that these are averages only. Impacts are not good at homogenizing temperatures. An impact initially deposits a large fraction of its kinetic energy in a region comparable in size to the projectile itself. Shortly after a time measured by D/v_i, the projectile diameter D divided by its impact velocity v_i, the shock waves generated by the impact expand away from the impact site, accelerating the target material and depositing heat as they spread out and weaken. The heat is therefore mostly deposited in a region called the 'isobaric core' whose shape is initially approximately that of an immersed sphere tangent to the surface of the target. Outside of this region the shock pressure, and therefore the amount of heat deposited, falls off rapidly, generally as more than the cube of the distance from the impact (Pierazzo *et al.*, 1997). A velocity field that is established by the spreading shock wave accompanies this heat deposition. The moving material generally opens a crater whose size and form depends on the relative importance of gravity and strength in the crater excavation. In general, about half of the hot, isobaric core is ejected from the impact site, to spread out beyond the crater rim, while the other half remains in the distorted target beneath the crater floor (i.e., for impacts that do not vaporize a large volume of the target, which is the case for all accretional impacts on Earth-sized planets). The major part of the kinetic energy of the impact is thus converted to heat in a roughly hemispherical region centered on the crater. This hot zone extends to a depth of only a few projectile diameters.

For small impacts, generally those of objects less than a kilometer in diameter, the heat is deposited so close to the surface that a major fraction is radiated to space before the next similar-size impact occurs (Melosh, 1990). Larger impactors deposit more of their energy deeper in the planet, up to the truly gigantic impacts of objects comparable in size to the growing Earth, which may deposit their energy over an entire hemisphere. Nevertheless, detailed computations show that this energy is not homogeneously distributed over the target Earth. Later processes, such as the re-impact of large fractions of the projectile (seen in some of the Moon-forming scenarios: Canup, 2004), or thermal convection of the mantle driven by a suddenly heated core, are needed to homogenize the heat input. Impact heating is thus characterized by large initial temperature variations: the part of the Earth near the impact site becomes intensely hot while more distant regions remain cold. Averages, therefore, tell only a small part of the overall story: the aftermath of heating by a large impact is characterized by strong temperature gradients and the evolution of the planet may be dominated by contrasts between very hot and cold, mostly unaffected, portions of the growing Earth.

9.03.2.2.3 Heating through the reduction of gravitational potential energy

Although the energies involved in late-stage impacts imply the formation of a magma ocean, such an ocean may not reach the CMB, because the solidus temperature of mantle material is a strong function of pressure (see **Figure 9(b)** below). The mechanical properties of the magma ocean, which control the rate of iron transport across the ocean, change dramatically when the melt fraction drops below ≈60% (Solomatov, 2000; *see also* Chapter 9.04). The effective base of the magma ocean occurs at this rheological transition. Descending iron droplets will tend to pond at this interface. However, the resulting iron layer is still denser than the underlying (mantle) material and will therefore tend to undergo further transport towards the center of the planet. The transport mechanism might be percolation through a partially molten mantle, or the motion of larger iron bodies via brittle fractures (dyking) or through a viscously deformable mantle (diapirism). These different mechanisms are discussed in Stevenson (1990) and will be addressed in more detail in Section 9.03.2.3.

The redistribution of mass involved with the descent of iron toward the center of the planet results in a release of gravitational energy. Because the gravitational energy change only depends on the initial and final density distributions, the mechanism by which the iron is transported is of only secondary importance. The extent to which the iron, rather than the surrounding mantle material, is heated depends on the rate of transport (rapid for diapirs or dykes, slower for percolation) but the total energy released

would be the same. The magnitude of the heating can be large, and may be calculated as follows.

Consider a uniform, thin layer of iron at the base of the magma ocean, overlying a mantle and core (Figure 4). The top and bottom of the iron layer and the underlying core are at radii R_o, $R_m = (1-\varepsilon)R_o$ and $R_c = \beta R_o$, respectively, where ε is a measure of the thickness of the iron layer ($\varepsilon << 1$) and β is a measure of the initial core radius. After removal of iron to the centre, whether by diapirism, dyking, or percolation, the core will have grown and the situation will have a lower potential energy. The difference in potential energy may be calculated and used to infer the mean temperature change in the final core, assuming that all the potential energy is converted to core heat (e.g., Solomon, 1979). For the specific case of a constant core density twice that of the mantle, it may be shown that the mean temperature change of the entire post-impact core is given by

$$\Delta T = \frac{\pi G \rho_c R_o^2}{\beta^3 C_p (1 + 3\varepsilon\beta^{-3})} \times \left[\frac{1}{10}\beta^5\left((1 + 3\varepsilon\beta^{-3})^{5/3} - 1\right) + \frac{1}{2}\varepsilon - \beta^3\varepsilon\right] \quad [4]$$

Here C_p is the specific heat capacity of the core and ρ_c is the core density, and it is assumed that the core is well-mixed (isothermal). As before, the temperature change is a strong function of planetary size, specifically the radial distance to the base of the magma ocean R_o. The temperature change also depends on ε, which controls the mass of iron being delivered to the core, and the initial core radius R_c when $\beta > 0$. The temperature change goes to zero when $\beta = 1$, as expected, while when $\beta = 0$ (i.e., no initial core) the temperature change is essentially independent of the mass of iron delivered.

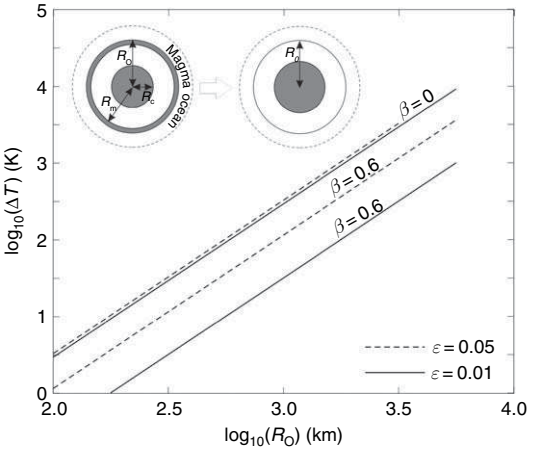

Figure 4 Temperature change due to iron layer descent, from eqn [4]. Here ε is a measure of the thickness of the iron layer being added to the core and is given by $1 - (R_m/R_o)$, while β is a measure of the initial core radius and is given by $\beta = R_c/R_o$.

Figure 4 shows the expected temperature change as a function of R_o plotted for different values of β and ε. It is clear that for Earth-sized planets, the addition of iron to the core by individual impacts can lead to core temperature increases of several hundred to a few thousand kelvin.

For example, consider two cases, appropriate to the Moon-forming impact (Canup and Asphaug, 2001): a $0.9M_e$ planet hit by a $0.1M_e$ impactor, and a $0.8M_e$ planet hit by a $0.2M_e$ impactor, all bodies having a core of density $10^4\,\mathrm{kg\,m^{-3}}$ and radius half the body radius. For magma oceans of depths 500 and 1000 km, respectively ($R_o = 5900$ and 5400 km), we obtain $\varepsilon = 0.0054$ and 0.0139, and $\beta = 0.52$ and 0.55. The core adiabat is roughly $1\,\mathrm{K\,km^{-1}}$, giving temperature increases of 2400 and 1900 K. The further increases from gravitational heating (eqn [4]) are 1250 and 2000 K, respectively. Thus, the post-impact core temperature is likely to have increased by 3500–4000 K from the temperature it attained at the base of the magma ocean. Because the base of the magma ocean is estimated to be in the range 2500–4000 K (Section 9.03.3.2), the initial core temperature was probably at least 6000 K, sufficient to cause substantial lower-mantle melting.

This estimate is only approximate, because of the assumptions made (e.g., no transfer of heat to the mantle) and the fact that the Earth probably suffered several comparably sized impacts. However, the result is important because the initial temperature contrast between the core and the lowermost mantle determines the initial CMB heat flux, and thus the ability of the core to generate a dynamo.

9.03.2.3 Differentiation Mechanisms

A crucial question is at what stage during the accretion history did core–mantle differentiation actually occur and how long did the process take? These questions depend on the thermal history of the accreting body which, in turn, determines the physical mechanisms by which metal and silicate separate. The physics of differentiation have been reviewed previously by Stevenson (1990) and Rushmer *et al.* (2000) and here we provide an updated account. Differentiation occurs because of the large density contrast between silicates and metal, but the rate at

which it occurs depends on the length scales and properties of the phases involved. Considering the current size of the Earth, the segregation process involved the transport of metal through the protomantle over length scales of up to almost 3000 km. As reviewed by Stevenson (1990), the process involved the transport of liquid metal through either solid (crystalline) silicates or through partially or fully molten silicate (i.e., in a magma ocean). The former mechanism is possible because iron (plus alloying elements) has a lower melting temperature than mantle silicates, so that liquid iron can coexist with solid silicates. In contrast, the separation of solid metal from solid silicate is too sluggish to have been a significant process during core formation (Stevenson, 1990). Identifying whether metal separated from solid or molten silicates during core formation clearly provides information about the early thermal state of the planet. In addition, the separation mechanism may have affected the conditions and extent of chemical equilibration between metal and silicate and therefore affects mantle geochemistry, as discussed further below. Here we review recent results pertaining to core formation by (1) grain-scale percolation of liquid metal through crystalline silicates, (2) separation of molten metal from molten silicate in a magma ocean, and (3) descent of large (kilometer scale) diapirs of molten metal through crystalline silicate and/or transport by a fracture/dyking mechanism.

As discussed above, it seems likely that the final stages of Earth's accretion involved large impacts between previously differentiated objects which were at least partly molten. What happens in detail during these impacts is poorly understood. Hydrocode simulations of impacts (Cameron, 2000; Canup and Asphaug, 2001) show that the cores of the target and impactor merge rapidly, within a few free-fall timescales (hours), although a small fraction (typically <1%) of core material may be spun out into a disk. Unfortunately, the resolution of these simulations is on the order of 100 km, while the extent to which chemical re-equilibration occurs depends on length scales that are probably on the order of centimeters (Stevenson, 1990). Another approach to understanding this important question is presented in Section 9.03.2.3.2.

9.03.2.3.1 Percolation

Liquid metal can percolate through a matrix of polycrystalline silicates by porous flow provided the liquid is interconnected and does not form isolated pockets (Stevenson, 1990; Rushmer *et al.*, 2000). The theory is well developed for the ideal case of a monominerallic system consisting of crystals with isotropic surface energy (i.e., no dependence on crystallographic orientation). Whether the liquid is interconnected depends on the value of the wetting or dihedral angle (θ) between two solid–liquid boundaries that are intersected at a triple junction by a solid–solid boundary (**Figure 5**) (von Bargen and Waff, 1986; Stevenson, 1990). For $\theta < 60°$, the liquid is fully interconnected and can percolate through the solid irrespective of its volume fraction; under such conditions, complete metal–silicate segregation can occur efficiently by porous flow. In the case that $\theta > 60°$, the liquid forms isolated pockets when the melt fraction is low ($\leq$0.8%) and connectivity exists only when the melt fraction exceeds a critical value. This critical melt fraction is known as the connection boundary and ranges from 2% to 6% for dihedral angles in the range 60–85°. If the melt fraction lies above the connection boundary, the melt is interconnected and can percolate. However, as the melt fraction decreases due to percolation, a pinch-off melt fraction is reached below which interconnectivity is broken. At this point the remaining melt is stranded in the crystalline matrix. The pinch-off melt fraction lies slightly below

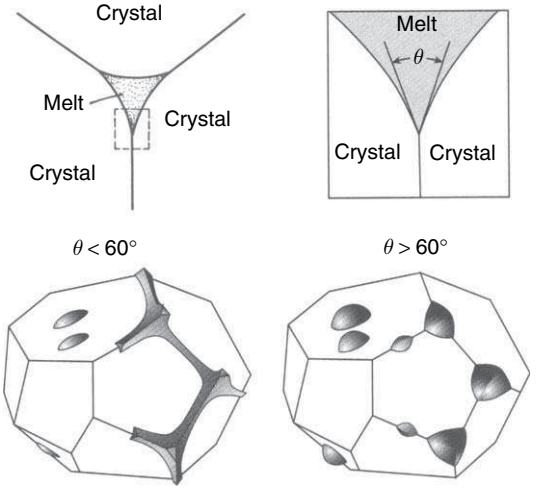

Figure 5 Relation between melt connectivity and dihedral angle in a polycrystalline aggregate containing a small amount of dispersed melt. The dihedral angle is defined in the top diagrams and the dependence of melt connectivity on the dihedral angle is shown in the lower diagrams. Note that an ideal case is shown here in which the crystals have an isotropic surface energy. Adapted from Stevenson DJ (1990) Fluid dynamics of core formation. In: Newsom HE and Jones JH (eds.) *Origin of the Earth*, pp. 231–250. New York: Oxford University Press.

the connection boundary and ranges from 0% to 4.5% for dihedral angles in the range 60–85°. The dependence of the pinch-off boundary on dihedral angle has been formulated theoretically as $0.009(\theta - 60)^{0.5}$ for values of θ in the range 60–100° (von Bargen and Waff, 1986). Yoshino *et al.* (2003) have shown, through electrical conductivity measurements, that the percolation threshold for Fe–S melt in an olivine matrix is approximately 5 vol.%. This result suggests that core formation could have occurred by percolation under hydrostatic conditions (see below) but ~5 vol.% metal would have been stranded in the mantle. In fact, 5 vol.% may be a lower bound on the amount of stranded metal because the percolation threshold theory was developed assuming that the liquid is uniformly and finely dispersed throughout the crystalline matrix (von Bargen and Waff, 1986). However, due to the minimization of surface energy, textures might evolve over long time periods (relative to normal experimental timescales of hours to days) such that the liquid becomes concentrated in pools that are widely dispersed and relatively large, in which case the percolation threshold could be much greater than 5 vol.% (Stevenson, 1990; Walte *et al.*, 2007).

The effects of crystal anisotropy and crystal faceting are not taken into account by the above theory (which is based on surface energies being isotropic). It has been argued that the effects of crystal anisotropy and crystal faceting reduce permeability (Faul, 1997; Laporte and Watson, 1995; Yoshino *et al.*, 2006); however, there is no experimental evidence to suggest that such effects are significant for liquid metal–silicate systems relevant to core formation.

The dihedral angle θ depends on the energies of the respective interfaces that intersect at a triple junction that is occupied by a melt pocket (**Figure 5**):

$$\theta = 2\cos^{-1}\left(\frac{\gamma_{ss}}{2\gamma_{sl}}\right) \quad [5]$$

where γ_{sl} is the solid–liquid interfacial energy and γ_{ss} is the solid–solid interfacial energy. Note that, as emphasized above, this expression is based on the assumption that interfacial energies are independent of crystal orientation and that stress is hydrostatic. When considering metal–silicate systems that are applicable to core formation, the interfacial energies, and therefore the dihedral angle, can be affected by (1) the structure and composition of the crystalline phase, (2) the structure and composition of the liquid metal alloy, and (3) temperature and pressure. Dihedral angles in metal–silicate systems relevant to core formation and the effects of the above variables have been investigated experimentally in recent years (Ballhaus and Ellis, 1996; Minarik *et al.*, 1996; Shannon and Agee, 1996, 1998; Gaetani and Grove, 1999; Holzheid *et al.*, 2000a; Rose and Brenan, 2001; Takafuji *et al.*, 2004; Terasaki *et al.*, 2005, 2007a, 2007b). These studies, performed on a range of different starting materials at pressure–temperature conditions up to those of the lower mantle, now enable the most important factors that control dihedral angles in metal–silicate systems to be identified.

The effects of pressure, temperature, and the nature of the silicate crystalline phase appear to be relatively unimportant, at least up to ~23 GPa. For example, through experiments on the Homestead meteorite, Shannon and Agee (1996) found that dihedral angles have an average value of 108° and remain essentially constant over the pressure range 2–20 GPa, irrespective of the dominant silicate mineral (e.g., olivine or ringwoodite). However, their subsequent study of the Homestead meteorite under lower-mantle conditions (25 GPa), suggests that dihedral angles decrease to ~71° when silicate perovskite is the dominant silicate phase (Shannon and Agee, 1998).

The most important parameter controlling dihedral angles is evidently the anion (oxygen and/or sulfur) content of the liquid metal phase. The reason is that dissolved O and S act as 'surface-active' elements in the metallic melt and thus reduce the solid–liquid interfacial energy (e.g., Iida and Guthrie, 1988). Dissolved oxygen, in particular, makes the structure of the metal more compatible with that of the adjacent silicate, thus reducing the interfacial energy and promoting wetting.

In a recent review, Rushmer *et al.* (2000, figure 4) showed that dihedral angles decrease from 100–125° to 50–60° as the anion to cation ratio, defined as $(O + S)/(Fe + Ni + Co + Mn + Cr)$, increases from ~0.3 to ~1.2. Based on their data compilation, only metallic melts with the highest contents of O and S are wetting ($\theta < 60°$). Recently, the effects of the anion content of the metallic liquid were investigated systematically in the stability fields of olivine and ringwoodite by Terasaki *et al.* (2005) through a study of dihedral angles in the system Fe–S–$(Mg, Fe)_2SiO_4$ in the pressure range 2–20 GPa. By varying the FeO content of the silicate phase ($Fe\# = FeO/(FeO + MgO) = 0.01$–$0.44$), the oxygen fugacity, which controls the O content of the metal, could be varied over a wide range. They confirmed the importance of the anion content of the liquid phase and showed that the effect of dissolved oxygen is greater than that of dissolved S (**Figure 6**). Because

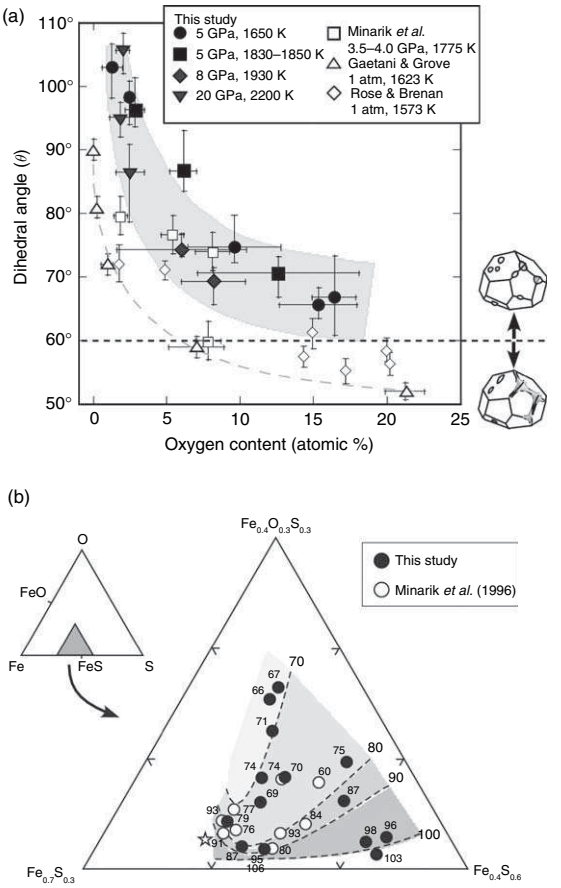

Figure 6 Dihedral angles in aggregates of olivine (≤8 GPa) and ringwoodite (20 GPa) containing several vol.% Fe–FeS melt as a function of the melt composition. (a) Dihedral angle as a function of the oxygen content of the Fe-alloy liquid. As the oxygen content increases, the structures of the silicate and liquid Fe alloy become more similar with the result that both the interfacial energy and the dihedral angle decrease. (b) Effects of O and S contents of the Fe-alloy liquid on dihedral angles. The data points are plotted on a triangular section of the Fe–O–S system and each data point is labeled with the dihedral angle. The dashed lines are contours of constant dihedral angle. These results suggest that the effect of dissolved O on the dihedral angle is greater than that of dissolved S. Reproduced from Terasaki H, Frost DJ, Rubie DC, and Langenhorst F (2005) The effect of oxygen and sulphur on the dihedral angle between Fe–O–S melt and silicate minerals at high pressure: Implications for Martian core formation. *Earth and Planetary Science Letters* 232: 379–392 (doi:10.1016/j.epsl.2005.01.030), with permission from Elsevier.

the oxygen content of the metallic liquid decreases with pressure up to 10–15 GPa (Rubie *et al.*, 2004; Asahara *et al.*, 2007), dihedral angles increase with increasing pressure in this range. Terasaki *et al.* (2007a) showed that for metallic liquids with a high O + S content, dihedral angles lie below 60° at pressures below 2–3 GPa, depending on the FeO content of the silicate phase. Percolation could therefore contribute significantly to core formation in planetesimals during the early stages of heating before the temperatures reach the silicate solidus.

Based on a recent study of liquid Fe + silicate perovskite at 27–47 GPa and 2400–3000 K, Takafuji *et al.* (2004) have suggested that dihedral angles decrease to ~51° under deep-mantle conditions. This result may be consistent with recent results which show that the solubility of oxygen in liquid Fe increases strongly with temperature and weakly with pressure above 10–15 GPa (Asahara *et al.*, 2007). However, the study of Takafuji *et al.* (2004) was performed using a laser-heated diamond anvil cell (LH-DAC), in which samples are exceedingly small and temperature gradients are very high. Furthermore, dihedral angles had to be measured using transmission electron microscopy – which is far from ideal for obtaining good statistics. This preliminary result there awaits confirmation from further studies. In addition, in a study of wetting in a similar system at the lower pressures of 25 GPa, Terasaki *et al.* (2007b) found that the dihedral angle increases with the $FeSiO_3$ component of silicate perovskite but failed to find any obvious correlation with the oxygen content of the metal liquid.

In summary, experimental results for systems under hydrostatic stress show that dihedral angles significantly exceed the critical angle of 60° at pressures of 3–25 GPa in chemical systems that are relevant for core formation in terrestrial planets. This means that, for percolation under static conditions, at least several vol.% metal would have been stranded in the mantle – which is inconsistent with the current concentration of siderophile elements in the mantle (see Section 9.03.3.2). Efficient percolation can occur at low pressures (<3 GPa) when the S and O contents of the metal are very high (i.e., close to the Fe–S eutectic) but such conditions are not applicable to core formation in a large planet such as the Earth. There is a preliminary indication that efficient percolation ($\theta < 60°$) may be a feasible mechanism under deep lower-mantle conditions but this result awaits confirmation.

When dihedral angles significantly exceed 60°, experimental evidence suggests that liquid metal can separate from crystalline silicates when the material is undergoing shear deformation due to nonhydrostatic stress (Bruhn *et al.*, 2000; Rushmer *et al.*, 2000; Groebner and Kohlstedt, 2006; Hustoft

and Kohlstedt, 2006). The most recent results indicate that ~1 vol.% liquid metal remains stranded in the silicate matrix so that reasonably efficient percolation of liquid metal, with percolation velocities on the order of 150 km yr^{-1}, might occur in crystalline mantle that is undergoing solid-state convection (Hustoft and Kohlstedt, 2006). There are, however, two potential problems with this shear-induced percolation mechanism. First, experiments have been performed at high strain rates (10^{-2} to 10^{-5} s^{-1}) and it is uncertain if the mechanism would also be effective at much lower strain rates. This is a consequence of the fact that at high strain rates the solid crystals do not deform appreciably and so can generate pore space by dilatent expansion of the crystal–melt mixture. At much lower strain rates the crystals can accommodate shear by deformation and so may greatly reduce the interconnections available for liquid-phase percolation. Second, the conversion of potential energy to heat during percolation of iron liquid in a planet the size of Earth might be sufficient to melt the silicates and thus change the mechanism to the one discussed in the next section (see Section 9.03.2.2.3).

9.03.2.3.2 Metal–silicate separation in a magma ocean

According to the results of calculations of the energy released by giant impacts, it is clear that the collision of a Mars-sized body with the proto-Earth would have resulted in the melting of a large part of, or even the entire planet (Section 9.03.2.2.2). In the case of partial melting, although the distribution of melt may initially have been concentrated on the side affected by the impact, isostatic readjustment would have led rapidly to the formation of a global magma ocean of approximately uniform depth (Tonks and Melosh, 1993). An important, and presently unresolved, question is whether this isostatic adjustment takes place on a timescale longer or shorter than that of iron separation. The mechanics of separation and chemical equilibration is quite different if the isostatic adjustment is much slower than iron separation, because then the melt region is not a global ocean of approximately uniform depth, but a restricted 'sea' that is both hotter and deeper than the ocean that eventually develops. This question is further raised below in Section 9.03.3.2.3.

Because of the large density difference between liquid iron and liquid silicate, magma ocean formation provides a rapid and efficient mechanism for the separation of these two phases. Here we examine the physics of metal–silicate separation in some detail because of the consequences for interpreting mantle geochemistry, as discussed below in Section 9.03.3.2.

A fundamental property that controls the dynamic behavior of a deep magma ocean is the viscosity of ultramafic silicate liquid. The viscosity of peridotite liquid has been determined at 2043–2523 K and 2.8–13.0 GPa by Liebske *et al.* (2005). Their results (**Figure 7**) show that viscosity increases with pressure up to 9–10 GPa and then decreases to at least 13 GPa (Reid *et al.*, 2003, found a similar trend for $CaMgSi_2O_6$ liquid). Based on a study of the self-diffusion of O and Si in silicate liquid, viscosity is expected to increase again at pressures above 18 GPa (Schmickler *et al.*, 2005). The transient decrease in viscosity in the pressure range 9–18 GPa may be caused by pressure-induced coordination changes (e.g., formation of fivefold and sixfold coordinated Si) in the melt structure (Liebske *et al.* 2005).

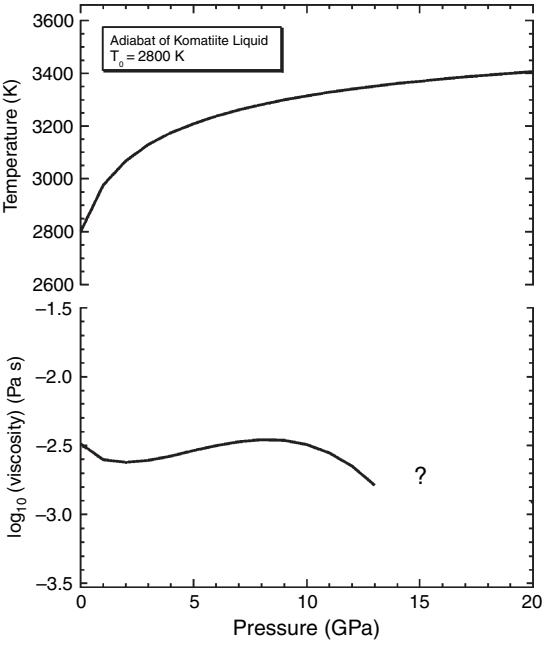

Figure 7 The viscosity of the upper part of a peridotitic magma ocean that has a total depth of ~1800 km (bottom). The viscosity is shown only to a depth of ~400 km because the existing experimental data cannot be extrapolated reliably to higher pressures. Based on results of Schmickler *et al.* (2005), the viscosity likely increases again above ~18 GPa. The viscosity profile is based on the adiabat shown in the top part of the figure. Reproduced from Liebske C, Schmickler B, Terasaki H, *et al.* (2005) Viscosity of peridotite liquid up to 13 GPa: Implications for magma ocean viscosities. *Earth and Planetary Science Letters* 240: 589–604, with permission from Elsevier.

Unfortunately, it is currently not possible to extrapolate these experimental results reliably in order to make predictions of melt viscosities at pressures significantly higher than 18 GPa; the large uncertainties involved in doing this are illustrated by Liebske *et al.* (2005, figure 7).

On the basis of the experimental data of Liebske *et al.* (2005), the viscosity of a magma ocean, at least to a depth of ~500 km, is estimated to lie in the range 0.01–0.003 Pa s, which is extremely low (for comparison, the viscosity of water at ambient conditions is 0.001 Pa s). Consequently, the Rayleigh number (which provides a measure of the vigor of convection) is extraordinarily high, on the order of 10^{27}–10^{32} (e.g., Solomatov 2000; Rubie *et al.*, 2003; *see* Chapter 9.04). This means that a deep magma ocean undergoes vigorous turbulent convection, with convection velocities on the order of at least a few meters per second. Using a simple parametrized convection model, the rate of heat loss can also be estimated, which leads to the conclusion that, in the absence of other effects (see below), the life time of a deep magma ocean on Earth is only a few thousand years (Solomatov, 2000).

What is the physical state of molten iron in a vigorously convecting magma ocean? Initially, iron metal may be present in states that range from finely dispersed submillimeter particles (as in undifferentiated chondritic material) to large masses that originated as cores of previously differentiated bodies (ranging in size from planetesimals to Mars-sized planets) that impacted the accreting Earth. In a molten system, very small particles tend to grow in size by coalescing with each other in order to reduce surface energy. Large molten bodies, on the other hand, are unstable as they settle and tend to break up into smaller bodies. A crucial question concerns the extent to which an impacted core breaks up and becomes emulsified as it travels through the target's molten mantle (see Stevenson (1990), Karato and Murthy (1997), and Rubie *et al.* (2003) for discussions of this issue). Hallworth *et al.* (1993) noted that laboratory-scale turbidity currents travel only a few times their initial dimension before being dispersed by turbulent instabilities). Such a core will experience both shear (Kelvin–Helmholtz) and buoyancy (Rayleigh–Taylor) instabilities. These processes operate at different length scales (R–T instabilities are small-scale features; see Dalziel *et al.*, 1999), but both processes will tend to break the body up until a stable droplet size is reached at which surface tension inhibits further break-up. The stable droplet size can be predicted using the dimensionless Weber number, which is defined as

$$W_e = \frac{(\rho_m - \rho_s) d v_s^2}{\sigma} \quad [6]$$

where ρ_m and ρ_s are the densities of metal and silicate respectively, d is the diameter of metal bodies, v_s is the settling velocity, and σ is the surface energy of the metal–silicate interface (Young, 1965). A balance between coalescence and breakup is reached when the value of W_e is approximately 10: when the value is larger than 10, instabilities cause further breakup to occur and when it is less than 10, coalescence occurs. The settling velocity v_s is determined using Stokes' law when the flow regime is lamellar or an equation that incorporates a drag coefficient when the flow around the falling droplet is turbulent (Rubie *et al.*, 2003). Both the settling velocity and the droplet size depend on silicate melt viscosity. For likely magma ocean viscosities and assuming a metal–silicate surface energy of 1 N m^{-1} (which is not well constrained – see Stevenson 1990), the droplet diameter is estimated to be ~1 cm and the settling velocity ~0.5 m s^{-1} (**Figure 8**; Rubie *et al.*, 2003, see also Stevenson (1990) and Karato and Murthy (1997)).

Having estimated the stable size of metal droplets, the next question is how quickly does a large mass of metal (e.g., 50–500 km in diameter) become emulsified and break up into a 'rain' of small droplets of stable diameter? Although the process is currently not well understood, Rubie *et al.* (2003) argued that emulsification should occur within a falling distance equal to a few times the original diameter of the body. Thus, the cores of all, except perhaps the largest, impacting bodies probably experienced a very large degree of emulsification.

The primary importance of emulsification is that it determines the degree to which chemical and thermal re-equilibration occurs (Karato and Murthy, 1997; Rubie *et al.*, 2003). Because thermal diffusivities are higher than chemical diffusivities, thermal equilibrium is always reached first. For typical settling velocities, iron blobs on the order of ~0.01 m in diameter will remain in chemical equilibration with the surrounding silicate liquid as they fall (Rubie *et al.*, 2003). Droplets that are much larger (e.g., on the order of meters or more in diameter) will fall rapidly and will not remain in equilibrium with the adjacent silicate because diffusion distances are too large. The physical arguments for emulsification summarized here are supported by evidence for chemical equilibration from both Hf–W observations

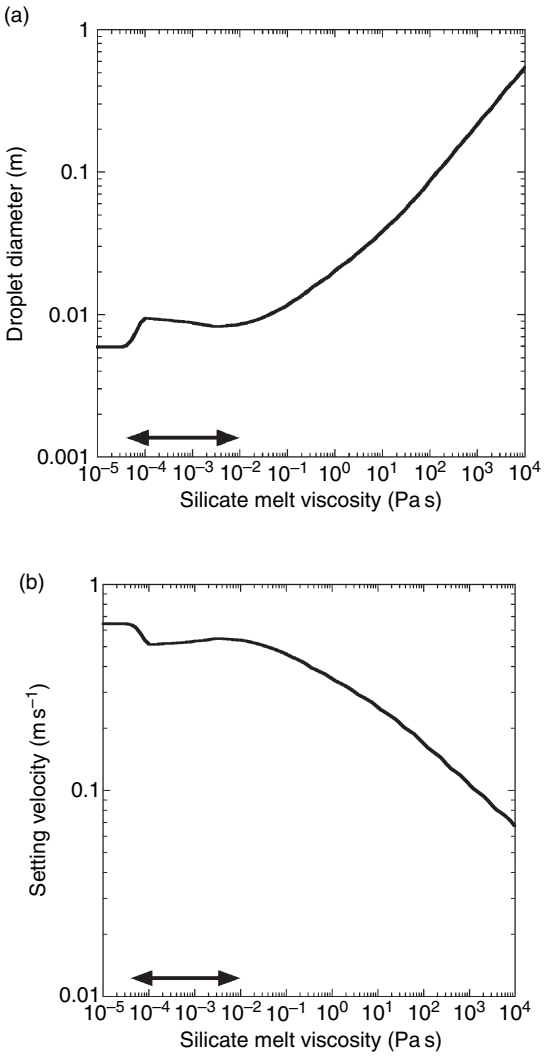

Figure 8 (a) Stable diameter of liquid iron droplets dispersed in a magma ocean as a function of silicate melt viscosity. The droplet diameter is calculated using the Weber number, as explained in the text. (b) Terminal settling velocity of liquid Fe droplets (of stable droplet diameter) as a function of silicate melt viscosity. The nonlinear trend arises from a transition from Stokes to turbulent flow at low viscosities. In both (a) and (b), the arrowed lines indicate the range of likely magma ocean viscosities. Reproduced from Rubie DC, Melosh HJ, Reid JE, Liebske C, and Righter K (2003) Mechanisms of metal-silicate equilibration in the terrestrial magma ocean. *Earth and Planetary Science Letters* 205: 239–255, with permission from Elsevier.

(Section 9.03.3.1) and siderophile element abundances in the mantle (Section 9.03.3.2). Since chemical equilibration of macroscale iron bodies is very slow, this apparent equilibration strongly suggests that the iron was present, at least to a large extent, as small dispersed droplets (Righter and Drake, 2003).

Because likely settling velocities ($\sim$0.5 m s^{-1}) of small iron droplets are much lower than typical convection velocities ($\sim$10 m s^{-1}), iron droplets may remained entrained for a significant time in the magma ocean and accumulation through sedimentation at the base of the ocean will be a slow and gradual process. The dynamics of the settling and accumulation processes are important because they determine the chemical consequences of core formation (e.g., siderophile element geochemistry), as discussed below in Section 9.03.3.2.3.

The time taken for a magma ocean to start to crystallize is an important parameter when evaluating metal–silicate equilibrium models, as discussed below (Section 9.03.3.2.3). The existence of an early, thick atmosphere has little effect on large incoming impactors, but may be sufficiently insulating that, by itself, it ensures a magma ocean (e.g., Matsui and Abe, 1986). The depth to the (rheologically determined) base of the magma ocean is determined by the point at which the adiabat crosses the geotherm defining a melt fraction of roughly 60% (Solomatov, 2000). The survival time of the magma ocean depends on both the atmosphere and whether or not an insulating lid can develop. In the absence of these two effects, the lifetimes are very short, of order 10^3 years (e.g., Solomatov, 2000; Pritchard and Stevenson, 2000). However, if a conductive lid develops, the lifetime may be much longer, of order 10^8 years (Spohn and Schubert, 1991), and similar lifetimes can arise due to a thick atmosphere (Abe, 1997). Thus the lifetime of magma oceans is currently very unclear. The Moon evidently developed a chemically buoyant, insulating crust on top of its magma ocean (Warren, 1985). However, it did so because at low pressures aluminium partitions into low-density phases, especially plagioclase. At higher pressures, Al instead partitions into dense garnet, in which case a chemically buoyant crust will not develop (e.g., Elkins-Tanton *et al.*, 2003). In the absence of chemical buoyancy, a solid crust will still develop, but will be vulnerable to disruption by impacts or foundering (Stevenson, 1989). The latter process in particular is currently very poorly understood, and thus the lifetime of magma oceans remains an open question. Fortunately, even the short-lived magma oceans persist for timescales long compared to most other processes of interest.

9.03.2.3.3 Diapirs and dyking

If percolation is not an effective mechanism, then differentiation may occur either by downwards migration of large iron blobs (diapirism) or by propagation of iron-filled fractures (dyking).

The transport of iron though crystalline mantle as large diapirs, 1–10 km in diameter or larger, has been discussed in detail by Karato and Murthy (1997). When liquid iron ponds as a layer at the base of a magma ocean (**Figure 9**), gravitational instabilities develop due to the density contrast with the underlying silicate-rich material and cause diapir formation. Their size and rate of descent through the mantle depend on the initial thickness of the metal layer and the viscosity of the silicate mantle. Clearly gravitational heating will be important and will facilitate diapir descent by reducing the viscosity of the adjacent mantle. In contrast to magma ocean segregation, there will be no significant chemical exchange between metal and silicate, chemical disequilibrium will result and siderophile element abundances in the mantle cannot be a consequence of this mechanism (Karato and Murthy, 1997; *see also* Chapter 8.12).

Liquid iron ponded at the base of the magma ocean may also, under the right conditions, sink rapidly toward the Earth's core by dyking. Although it may be supposed that the hot, but nevertheless crystalline, mantle underlying the magma ocean cannot support brittle cracks, numerical studies summarized in Rubin (1995) indicate that dykes can still form, so long as the contrast in viscosity between the fluid in the dyke and the surrounding host rocks is greater than 10^{11}–10^{14}. With a viscosity in the neighborhood of 10^{-2} Pa s, liquid iron is thus expected to form dykes if the viscosity of the host rock exceeds 10^{9}–10^{12} Pa s. Given that the viscosity of the asthenosphere today is around 10^{19} Pa s, it is not unreasonable to expect the iron to reach the core via narrow dikes rather than as diapirs. In this case even less time is required for the rapidly descending iron to reach the core and thus less time for the iron to chemically equilibrate with the surrounding mantle. Indeed, even in the present Earth, Stevenson (2003) has proposed that masses of molten iron as small as 10^{8} kg (which would fill a cube about 25 m on a side) could travel from the Earth's surface to the core in about 1 week.

9.03.2.3.4 Summary and implications for chemical equilibration

A schematic illustration of how the various differentiation mechanisms might operate together is shown in **Figure 9**. Liquid metal separates rapidly from liquid silicate in a deep magma ocean and accumulates as ponded layers at the rheological base of the magma ocean. The ponded iron then migrates through the largely crystalline underlying mantle

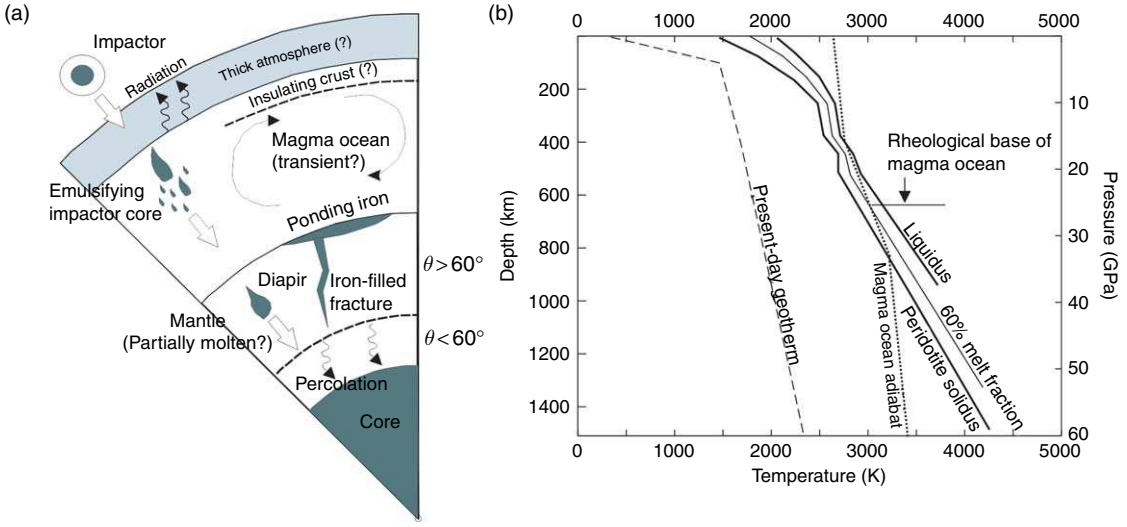

Figure 9 (a) Schematic diagram showing the various processes of metal–silicate segregation that could have operated during Earth accretion and core formation. The rheological base of the magma ocean is defined as the point at which the melt fraction drops below ~60% (Solomatov, 2000). (b) Temperature structure in the early Earth. The solidus curve in the lower mantle is uncertain (see Boehler, 2000), and the 60% melt fraction line is schematic, (b) Adapted from Walter MJ and Trønnes RG (2004) Early Earth differentiation. *Earth and Planetary Science Letters* 225: 253–269.

towards the proto-core by either percolation, diapirism, or dyking. According to experimental results summarized above, percolation is unlikely to be a completely efficient mechanism, even when catalyzed by shear deformation, but the mechanism may at least contribute to core formation. In addition, R–T instabilities develop at the base of the ponded layer and result in diapir formation. Given a sufficiently large viscosity contrast between liquid iron and the early silicate mantle, the dyking mechanism could also be important.

Despite the rapid transit times associated with falling iron drops and the somewhat longer timescales of percolative flow, the inferred length scales are small enough that complete chemical equilibration is expected. Conversely, descending iron diapirs are sufficiently large that chemical equilibrium is expected to be negligible (Karato and Murthy, 1997). Thus, the different differentiation mechanisms have very different chemical consequences. However, the magnitude of these chemical effects also depends on the relative abundances: a late passage of 1% core material through the mantle may well have a strong effect on mantle siderophile element abundances (e.g., W or Pt), but will have little effect on major element concentrations (e.g., oxygen) simply because the core material will become saturated and thus transport insignificant amounts of these more-abundant elements.

9.03.3 Observational and Experimental Constraints

Having discussed our theoretical expectations of accretion and core-formation processes, we will now go on to discuss the extent to which observations and experimental data may be used to differentiate between the various theoretical possibilities. Excellent summaries of many of these observations and experimental results may be found in Halliday (2003) and in the volume edited by Canup and Righter (2000).

9.03.3.1 Core-Formation Timescales

An extremely important development in recent years has been the recognition that some isotopic systems provide an observational constraint on core-formation timescales, and thus planetary accretion rates. The most useful isotopic system is Hf–W (Harper and Jacobsen, 1996; Kleine *et al.*, 2002; Schoenberg *et al.*, 2002; Yin *et al.*, 2002; Halliday, 2004; Jacobsen, 2005; note that Hf–W measurements published prior to 2002 were erroneous and led to conclusions that are now considered to be incorrect). The U–Pb system is more problematic, but generates results which can be reconciled with the more robust Hf–W technique (Wood and Halliday, 2005).

The Hf–W chronometer works as follows. W is siderophile (i.e., 'metal loving'), while Hf is lithophile (it remains in silicates). Furthermore, ^{182}Hf decays to stable ^{182}W with a half-life of 9 My. If an initially undifferentiated object suddenly forms a core after all the ^{182}Hf has decayed, the W will be extracted into the core and the mantle will be strongly depleted in all tungsten isotopes. However, if core formation occurs early, while ^{182}Hf is live, then the subsequent decay of ^{182}Hf to ^{182}W will enrich the mantle in radiogenic tungsten compared with nonradiogenic tungsten. Thus, a radiogenic tungsten excess, or tungsten anomaly, in the mantle is a sign of early core formation. Furthermore, if the silicate:iron mass ratio and the mantle concentrations of Hf and W compared with undifferentiated materials (chondrites) are known, then the observed tungsten anomaly can be used to infer a single-stage core-formation age. In the case of the Earth, this single-stage age is roughly 30 My (Jacobsen, 2005), while the Hf–W age of the Moon suggests that the last giant impact experienced by the Earth occurred at 30–50 My (Halliday, 2004; Kleine *et al.*, 2005).

There are three characteristics of the Hf–W system which makes it especially suitable for examining core formation. First, the half-life is comparable to the timescale over which planets are expected to form. Second, there are few other processes likely to lead to tungsten fractionation and perturbation of the isotopic system, though very early crustal formation or neutron capture (Kleine *et al.*, 2005) can have effects. Finally, both Hf and W are refractory; certain other isotopic systems suffer from the fact that one or more elements (e.g., lead) are volatile and can be easily lost during accretion.

The fact that tungsten isotope anomalies exist in the terrestrial mantle imply that core formation was essentially complete before about five half-lives (50 My) had elapsed. Mars and Vesta have larger tungsten anomalies, indicating that core formation ended earlier on these smaller bodies (Kleine *et al.*, 2002). The timescales implied are compatible with the theoretical picture of planetary accretion described in Section 9.03.2.1. The simple model of a single core-formation event is of course a

simplification of the real picture, in which the bulk of the core mass is added during stochastic giant impacts. However, more complicated models, in which the mass is added in a series of discrete events, do not substantially alter the overall timescale derived.

The observed tungsten anomaly depends mainly on the timescale over which the core forms, the relative affinities of Hf and W for silicates, and the extent to which the cores of the impactors re-equilibrate with the target mantle. The relative affinities of Hf and W can be determined, in a time-averaged sense, by measuring the present-day concentrations of these elements in the mantle. These affinities (i.e., the partition coefficients) may have varied with time, due to changing conditions (P, T, oxygen fugacity f_{O_2}) in the Earth. Although the dependence of the partition coefficients on these variables is known (e.g., Righter, 2003), how conditions actually evolved as the Earth grew is very poorly understood (e.g., Halliday, 2004). This caveat aside, if one accepts that the accretion timescales determined by numerical accretion models are reasonable, these models can then be used to investigate the extent to which re-equilibration must have occurred.

Figure 10 shows examples of the tungsten anomalies generated from numerical models of late-stage accretion (Nimmo and Agnor 2006). **Figure 10(b)** assumes that undifferentiated bodies undergo differentiation on impact, and that the bodies' cores then merge without any re-equilibration. In this case, the tungsten anomaly of a body is set by the mass-weighted average of the anomalies generated when each constituent planetesimal differentiated. Bodies made up of early colliding planetesimals tend to be bigger, and also have higher tungsten anomalies. The tungsten anomalies generated for Earth-mass bodies are much larger than those actually observed. **Figure 10(a)** shows results from the same accretion simulation, but now assuming that during each impact the core of the impactor re-equilibrates with the mantle of the target. This re-equilibration drives down the tungsten anomaly during each impact, and results in lower tungsten anomalies for large bodies than for small ones. The measured tungsten anomalies of Earth, Mars, and the HED parent body (probably Vesta) are all compatible with this mantle re-equilibration scenario. Thus, assuming that the accretion timescales generated by the simulations are correct, the Hf–W data suggest that even the largest impacts result in complete or near-complete equilibration of the impactor's core with the target's mantle. This conclusion in turn places constraints on the physics of these very large impacts and, in particular, suggests that emulsification of the impacting core occurs as it travels through the magma ocean (see also Section 9.03.2.3.2).

Although **Figure 10** only models the late stages of accretion, this is the stage when most of the Earth's mass is added. If re-equilibration occurs, earlier isotopic signatures will be overprinted. However, if core merging takes place, the overall signature will be set

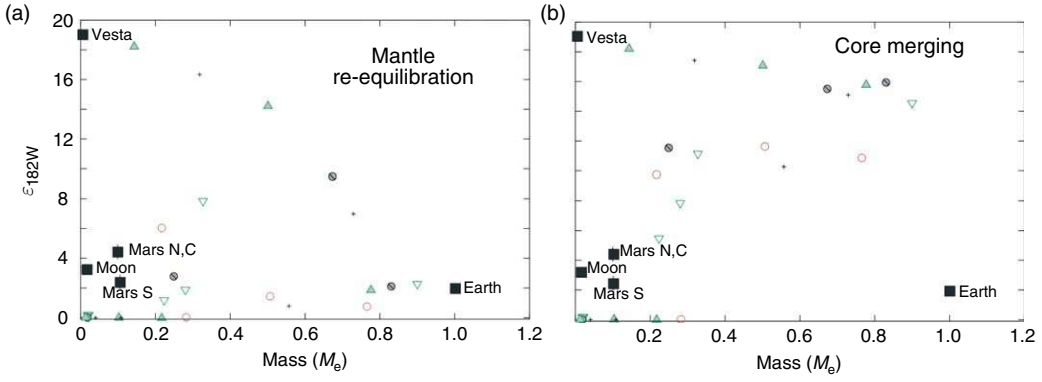

Figure 10 Isotopic outcomes of core formation based on N-body accretion codes. M_e is the mass of the final bodies in Earth masses, ε_{182W} is the final tungsten anomaly. Black squares are the observed values, tabulated in Jacobsen (2005) (Mars has two values because different meteorite classes give different answers). Colored symbols are the model results. Differentiation is assumed to occur when a body first collides with another object. (a) Outcome assuming that the impactor core re-equilibrates with the mantle of the target (a scenario favored if emulsification occurs). (b) Outcome assuming that the impactor core merges with the target core without any re-equilibration. Reproduced from Nimmo F and Agnor CB (2006) Isotopic outcomes of N-body accretion simulations: Constraints on equilibration processes during large impacts from Hf-W observations. *Earth and Planetary Science Letters* 243: 26–43, with permission from Elsevier.

by the time that the accreting objects differentiate. Since it appears that at least some bodies have differentiated very early and, in the case of Vesta, have correspondingly high tungsten anomalies (Kleine *et al.*, 2002), **Figure 10(b)** probably underestimates the tungsten anomalies that would result if re-equilibration did not occur.

Finally, because the early history of the core and the mantle are intimately coupled, there are some isotopic systems governed by mantle processes which are also relevant to core-formation timescales. In particular, the nonchondritic ^{142}Nd isotope signature of the Earth's upper mantle has been used to argue for global melting of the mantle within 30 My of solar system formation (Boyet and Carlson, 2005). This constraint is entirely consistent with the core-formation timescale derived above; however, Ba isotope measurements have been used to argue that the Earth as a whole is not chondritic (Ranen and Jacobsen, 2006), thus making the ^{142}Nd measurements more difficult to interpret. Sm–Nd and Lu–Hf chronometers are also consistent with the solidification of a magma ocean with the first ~100 Myr of Earth's history (Caro *et al.*, 2005), and U–Pb dates have been interpreted as resulting from the final stage of magma ocean crystallization at about 80 Myr after solar system formation (Wood and Halliday, 2005). Xe-isotope data give a comparable time for loss of xenon from the mantle (e.g., Porcelli *et al.*, 2001; Halliday, 2003).

In summary, the Hf–W system is important for two reasons: it constrains the timescale over which core formation occurred, and it also constrains the extent of re-equilibration between core and mantle material. To obtain the pressure–temperature conditions under which this re-equilibration took place, it is necessary to look at other siderophile elements as well. Inferring the equilibration conditions is important both because constraints are placed on the early thermal state of both core and mantle, and because these conditions strongly influence the ultimate composition of the core.

9.03.3.2 Constraints from Siderophile Element Geochemistry

9.03.3.2.1 Introduction to siderophile element geochemistry

The primary geochemical evidence for core formation in the Earth is provided by a comparison of the composition of the Earth's silicate mantle with its bulk composition. Estimates of the composition of the mantle are based on numerous geochemical studies of mantle peridotites and are well established (e.g., McDonough and Sun, 1995; Palme and O'Neill, 2003), assuming of course that the mantle is homogeneous. Although the bulk composition of the Earth is not known precisely (O'Neill and Palme, 1998; Drake and Righter, 2002), it is often approximated by the composition of C1 carbonaceous chondrites, which are the most pristine (undifferentiated) relicts known from the early solar system. As seen in **Figure 11**, refractory lithophile elements (e.g., Al, Ca, Ti, Ta, Zr, and the rare earth elements, REE's) are present in the mantle in C1 chondritic concentrations, and their concentrations have therefore been unaffected by accretion or differentiation processes. Compared with the bulk composition of the Earth, the mantle is strongly depleted in (1) siderophile (metal-loving) elements that have partitioned into iron-rich metal during formation of the Earth's core (Walter *et al.*, 2000) and (2) volatile elements that are considered to have been partly lost during accretion. Note that some of the volatile elements are also siderophile (e.g., sulfur) so that current mantle concentrations can be the result of both core formation and volatility (for a full classification of depleted elements, see Walter *et al.*, 2000, **Table 1**). Siderophile elements that are unaffected by volatility are most valuable for understanding core formation and these include the moderately siderophile elements (MSEs) (e.g., Fe, Ni, Co, W, and Mo) and the highly-siderophile elements (HSEs), which include the platinum group elements (PGE's, e.g. Re, Ru, Rh, Os, Ir, Pd, Pt, and Au).

The degree of siderophile behavior is described for element M by the metal–silicate partition coefficient $D_M^{met-sil}$ which is defined as

$$D_M^{met-sil} = \frac{C_M^{met}}{C_M^{sil}} \quad [7]$$

where C_M^{met} and C_M^{sil} are the wt.% concentrations of M in metal and silicate, respectively. The MSEs are defined as having values (determined experimentally at 1 bar) of $D_M^{met-sil} < 10^4$, whereas HSEs have 1-bar values that are greater than 10^4 and can be, in the case of Ir for example, as high as 10^{10}. The boundary between siderophile and lithophile behavior is defined as $D_M^{met-sil} = 1$.

As discussed below, partition coefficients are a function of pressure and temperature. An additional controlling parameter, which is critical in the context of core formation, is oxygen fugacity, f_{O_2}. The effect

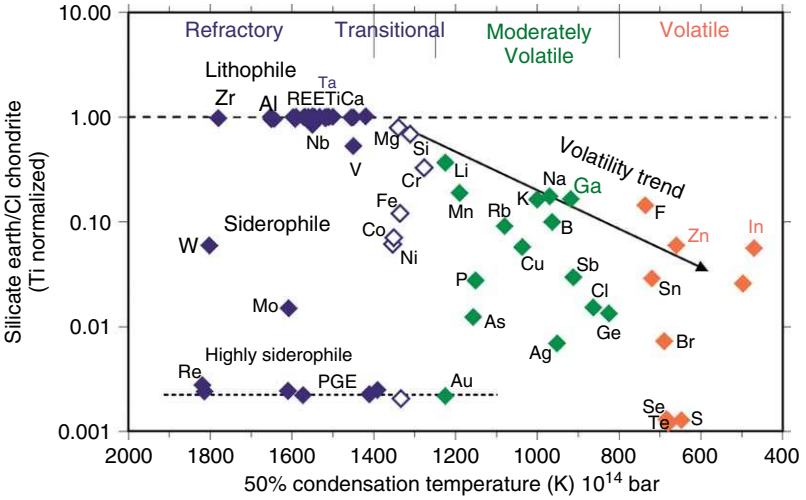

Figure 11 Element abundances of the Earth's mantle normalized to CI chondrite and the refractory element Ti (data after Palme and O'Neill, 2003) plotted against their 50% condensation temperatures as given by Wasson (1985). Note that the errors on these data points may be large (e.g. at least an order of magnitude for some volatile elements). Courtesy of Ute Mann.

of f_{O_2} on the partitioning of a siderophile element depends on its valence state when it is dissolved in the silicate phase, as can be understood by considering the following metal–silicate equilibrium:

$$\underset{\text{metal}}{M} + (n/4)O_2 = \underset{\text{silicate liquid}}{MO_{n/2}}$$

(e.g., Righter and Drake, 2003). Here M is the element of interest and n is its valence when it is dissolved in silicate liquid. Increasing the oxygen fugacity drives the equilibrium toward the right-hand side, thus increasing the concentration of M in the silicate liquid and reducing the value of $D_M^{met-sil}$. Typically, the dependence of $D_M^{met-sil}$ on f_{O_2}, pressure (P), and temperature (T) is expressed by a relationship of the form

$$\ln D_M^{met-sil} = a \ln fO_2 + b/T + cP/T + g \qquad [8]$$

where a is related to the valence state of M in the silicate liquid and b, c, and g are related to thermodynamic free energy terms which have generally assumed to be constants even when the P–T range of extrapolation is large (see Righter and Drake (2003)). In reality, these parameters are not likely to be constant over large ranges of pressure, temperature, and f_{O_2}. For example, the valence state of an element can change as a function of f_{O_2}. Pressure-induced changes in silicate melt structure may also cause a strong nonlinear pressure dependence at certain conditions (Keppler and Rubie, 1993; Kegler *et al.*, 2005). In addition to P, T, and f_{O_2}, the effects of additional factors, such as the composition/structure of the silicate melt and sulfur and carbon contents of the metal, may also need to be included empirically (Righter and Drake, 2003; Walter *et al.*, 2000).

For core formation, the value of f_{O_2} is constrained by the partitioning of Fe between the mantle and core and is estimated to have been 1 to 2 log units below the oxygen fugacity defined by the iron–wüstite (Fe-FeO or 'IW') buffer (which is abbreviated as IW-1 to IW-2).

Values of $D_M^{met-sil}$ for the core–mantle system lie in the range 13–30 for MSEs and 600–1000 for HSEs (for compilations of values, see Wade and Wood, 2005; Wood *et al.*, 2006). These values are much lower than experimentally determined 1-bar metal–silicate partition coefficients, in some cases by a few orders of magnitude, and show that the mantle contains an apparent 'overabundance' of siderophile elements. Possible explanations of this anomaly, the so-called 'excess siderophile element problem', form the basis of theories of how and under which conditions the Earth's core formed (e.g., Newsom, 1990; Righter, 2003), as described further in Section 9.03.3.2.2. An important additional constraint is provided by the observation that the HSEs are present in the mantle in approximately chondritic relative abundances (**Figure 12**), even though the experimentally determined 1-bar $D_M^{met-sil}$ values vary by orders of magnitude.

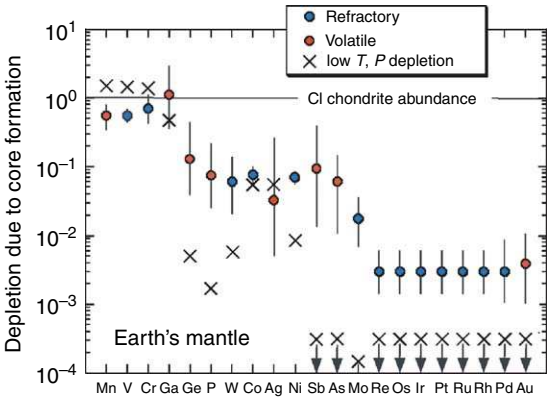

Figure 12 Depletion of siderophile elements in the Earth's mantle as the result of core formation. The siderophile elements are distinguished as being either refractory or volatile. The crosses show depletion values that would be expected on the basis of partitioning experiments performed at one bar and moderate temperatures (e.g., 1300°C); in the case of the highly-siderophile elements, the predicted values plot far below the bottom of the graph and are highly variable. The large discrepancies between the observed and calculated values shown here form the basis for the 'siderophile element anomaly'. For further details see Walter *et al.*, (2000). After Walter MJ, Newsom HE, Ertel W, and Holzheid A (2000). Siderophile elements in the Earth and Moon: Metal/silicate partitioning and implications for core formation. Reprinted from Canup RM and Righter K (eds.) *Origin of the Earth and Moon*, pp. 265–290. Tucson, AZ: University of Arizona Press; Courtesy of Michael Walter, with permission of the University of Arizona Press.

Important constraints on how the Earth's core formed are potentially provided by also considering the geochemical consequences of core formation in other planetary bodies. If the sizes of such bodies differ significantly from that of the Earth, pressure–temperature conditions of metal–silicate equilibration will also be different, thus enabling some of the theories detailed below (Section 9.03.3.2.2) to be tested. Estimates of the geochemical effects of core formation in Mars, Vesta, and the Earth's Moon are also based on comparisons of siderophile element concentrations in the mantles of these bodies with their likely bulk compositions (e.g., Treiman *et al.*, 1987; Righter and Drake, 1996; Walter *et al.*, 2000). Both bulk and mantle compositions are poorly constrained compared with the Earth. Mantle compositions are inferred from studies of SNC meteorites for Mars, the eucritic meteorites for Vesta and samples collected from the Moon's surface (Warren 1993; McSween, 1999). In all cases, the samples (e.g., lavas and cumulates) are the products of crustal differentiation processes and therefore mantle compositions have to be inferred by taking the effects of differentiation into account. In the case of the Moon, there is an additional problem because the petrogenesis of samples is poorly constrained because of their extremely small size (Warren, 1993).

Compared to the Earth's mantle, current assessments indicate that the Martian mantle is relatively depleted in Ni and Co, whereas concentrations of HSE's are similar. As in the Earth's mantle, the HSEs appear to be present in chondritic relative abundances (Kong *et al.*, 1999; Warren *et al.*, 1999; McSween, 1999; Jones *et al.*, 2003). The mantles of both the Moon and Vesta show relatively large depletions in most siderophile elements (Righter and Drake, 1996; Walter *et al.*, 2000). It is not possible in any of these cases to explain mantle siderophile element abundances by simple metal–silicate equilibrium at moderate pressures and temperatures, that is, based on 1-bar experimental data.

9.03.3.2.2 Core formation/accretion models

As described in the previous section, siderophile element concentrations are depleted in the Earth's mantle relative to chondritic compositions as a consequence of core formation (**Figures 11** and **12**). However, compared with predicted depletions based on element partitioning studies at 1 bar and moderate temperatures (e.g., 1300–1400°C) the concentrations of siderophile elements are too high (**Figure 12**; Wood *et al.*, 2006, Table 1). In the case of MSEs, the discrepancies are around 1–2 orders of magnitude. In the case of the HSEs, the discrepancies are on the order of 5–10 orders of magnitude.

The apparent overabundance of siderophile elements in the mantle has led to a number of core-formation hypotheses, most notably:

- metal–silicate equilibration at high pressures and temperatures,
- the late-veneer hypothesis,
- inefficient core formation, and
- addition of core material to the lower mantle.

We briefly review each of these hypotheses in turn.

9.03.3.2.2.(i) Metal–silicate equilibration at high pressure and temperature Murthy (1991) proposed that mantle siderophile element abundances could be explained if temperatures during core formation were extremely high. Although there were significant problems with the thermodynamic arguments on which this suggestion was based

(Jones *et al.*, 1992; O'Neill, 1992), metal–silicate equilibration at combined high temperatures and pressures may provide the explanation for at least the MSE abundances. This topic has been reviewed recently in detail by Walter *et al.* (2000), Righter and Drake (2003), and Wood *et al.* (2006).

Preliminary high-pressure studies produced results that were inconclusive in determining whether metal–silicate equilibration can explain the siderophile element anomaly (Walker *et al.*, 1993; Hillgren *et al.*, 1994; Thibault and Walter, 1995; Walter and Thibault, 1995). However, an early study of the partitioning of Ni and Co between liquid Fe alloy and silicate melt suggested that the metal–silicate partition coefficients for these elements reach values that are consistent with mantle abundances at a pressure of 25–30 GPa (**Figure 13(a)**; Li and Agee, 1996). This important result led to the idea (which has been disputed recently by Kegler *et al.*, 2005) that metal–silicate equilibration at the base of a magma ocean ~800 km deep can explain the mantle abundances of at least the MSEs (Li and Agee, 1996; Righter *et al.*, 1997). Since the late 1990s, there have been numerous subsequent studies of the partitioning of the MSEs (e.g., Li and Agee, 2001; O'Neill *et al.*, 1998; Gessmann and Rubie, 1998, 2000; Tschauner *et al.*, 1999; Righter and Drake, 1999, 2000, 2001; Chabot and Agee, 2003; Bouhifd and Jephcoat, 2003; Chabot *et al.*, 2005; Wade and Wood, 2005; Kegler *et al.*, 2005). A growing consensus emerging from such studies is that the pressures and temperatures required for metal–silicate equilibration may have been considerably higher than originally suggested. Estimated conditions are quite variable and range up to >4000 K and 60 GPa (**Table 3**; **Figure 14**). One of the reasons for the large scatter of P–T estimates is that, based on the current experimental data set and the associated uncertainties, a wide range of P–T–f_{O_2} conditions can satisfy mantle abundances of the MSEs (**Figure 14**). In addition, the difficulty of identifying a unique set of conditions is hardly surprising considering that core formation occurred over a protracted time period during accretion as the likely consequence of multiple melting events under a range of conditions.

The solubilities of HSEs in silicate liquid have been investigated extensively at 1 bar and moderate temperatures of 1300–1400°C (e.g., Ertel *et al.*, 1999, 2001; Fortenfant *et al.*, 2003a, 2006), whereas there have been only a few studies of the solubility or partitioning of HSE's at high pressure. All such studies are beset by a serious technical problem. The quenched samples of silicate liquid inevitably contain numerous metal micronuggets consisting of or rich in the element of interest, especially at low f_{O_2}, which make it very difficult to obtain reliable chemical analyses. Although it is normally considered that such nuggets were present in the melt at high temperature (e.g., Lindstrom and Jones, 1996; Holzheid *et al.*, 2000b), it has also been suggested that they form by exsolution from the silicate liquid during quenching (Cottrell and Walker, 2006). Depending on the interpretation adopted, greatly different results are obtained. So far, the solubilities of Pt and Pd in silicate liquid (Holzheid *et al.*, 2000b; Ertel *et al.* 2006; Cottrell and Walker, 2006), the metal–silicate partitioning of Re (Ohtani and Yurimoto, 1996) and the partitioning of Re and Os between magnesiowüstite and liquid Fe (Fortenfant *et al.*, 2003b) have been investigated at high pressure. The concentrations of Re and Pt in the mantle may possibly be explained by metal–silicate equilibration (Righter and Drake, 1997; Cottrell and Walker, 2006). However, the conclusion of the majority of these studies is that metal–silicate equilibration at high pressure is very unlikely to explain the concentrations of all HSEs in the mantle and, in particular, their chondritic ratios. In addition, based on studies of Martian meteorites, HSE abundances are similar in the mantles of both Earth and Mars (Warren *et al.*, 1999). This is difficult to explain by metal–silicate equilibration because, in planets of dissimilar sizes, P–T conditions of core formation should be quite different. Therefore, metal–silicate HSE partitioning results are generally interpreted to support the late-veneer hypothesis (see next section) for both Earth and Mars (e.g., Righter, 2005).

There are several problems with the simple concept of metal–silicate equilibration at the base of a magma ocean. First, the complete process of core formation in the Earth cannot be accomplished through a single event involving a magma ocean of limited depth (e.g., 800–1500 km). Several large impacts are likely to have occurred during accretion, each generating a magma ocean with different characteristics, while there may also have been a steady background flux of smaller impactors. Second, many of the proposed P–T conditions (e.g., 3750 K and 40 GPa) lie far (e.g. ~650 K) above the peridotite liquidus temperature (Wade and Wood, 2005; see **Figure 15**). The temperature at the base of a magma ocean should lie between the solidus and liquidus temperatures (**Figure 9(b)**); therefore, this observation appears to require that the metal ceased equilibrating with the silicate liquid far above the bottom of the magma ocean. Based on the arguments given above concerning emulsification (Section 9.03.2.3.2), this possibility is very unlikely. Finally, the

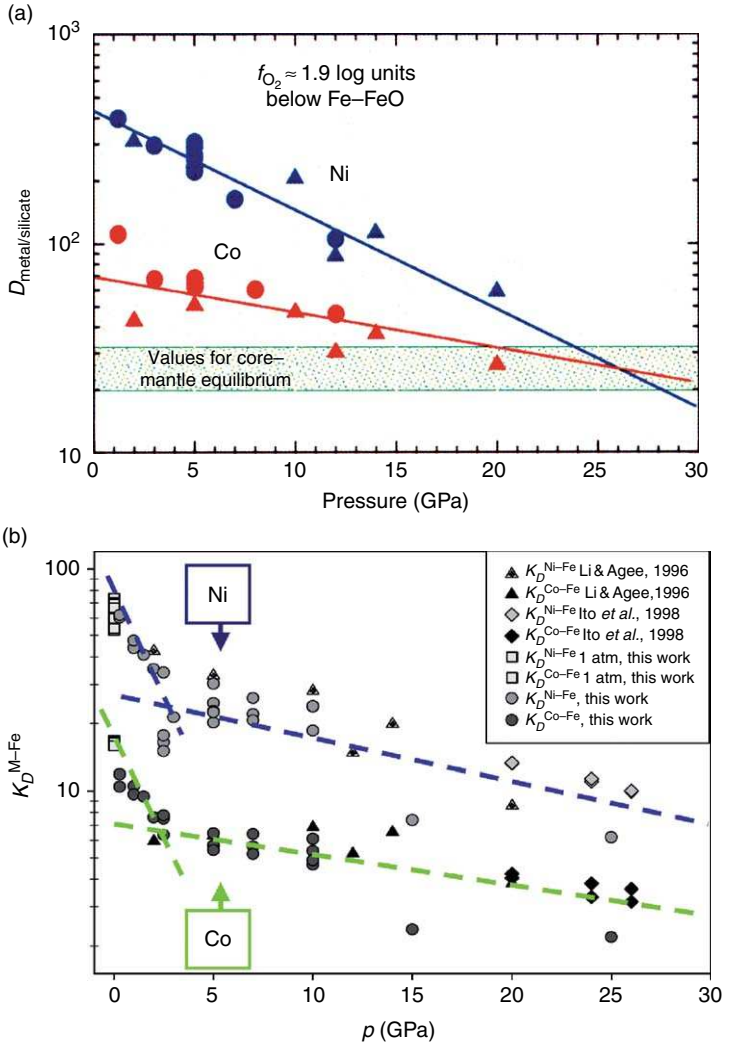

Figure 13 (a) Early experimental results on the effects of pressure on the partitioning of Ni (blue symbols) and Co (red symbols) between liquid Fe alloy and liquid silicate melt, at 2123–2750 K and f_{O_2} = IW-1.9, that led to the hypothesis of metal and silicate equilibrating during core formation at the bottom of a deep magma ocean. Triangles show data from Li and Agee (1996) and filled circles show data from Thibault and Walter (1995). (b) More recent results on the partitioning of Ni and Co show that the pressure dependence undergoes a pronounced change at ~3 GPa, probably because of pressure-induced structural changes in the silicate liquid (see Keppler and Rubie, 1993); above 3 GPa the pressure dependences for both Ni and Co are considerably weaker than the trends shown in (a). Here K_D^{M-Fe} is a distribution coefficient in which the partition coefficient has been normalized to Fe partitioning and is thus independent of f_{O_2}; in addition, the data have all been normalized to 2273 K by extrapolation. (a) Reprinted from Wood BJ, Walter MJ, and Wade J (2006) Accretion of the Earth and segregation of its core. *Nature* 441: 825–833, doi: 10.1038/nature 04763, with permission from Macmillan Publishers Ltd. (b) From Kegler P, Holzheid A, Rubie DC, Frost DJ, and Palme H (2005) New results of metal/silicate partitioning of Ni and Co at elevated pressures and temperatures. *XXXVI Lunar and Planetary Science Conference*, Abstract #2030.

assumption is made that a layer of ponded liquid iron can equilibrate chemically with the overlying convecting magma ocean (see **Figure 9(a)**). As discussed further below (Section 9.03.3.2.3) this is unlikely to be realistic and more complex metal–silicate fractionation models are required.

In order to overcome the first two problems listed above, Wade and Wood (2005) presented a model in which core formation occurs continuously during accretion. This is based on the metal–silicate partitioning of a range of elements, including Fe, Ni, Co, V, W, Nb, Cr, and Mn, assuming equilibration at the

Table 3 Metal–silicate equilibration conditions during core formation inferred from experimental studies of siderophile element partitioning

P(GPa)	T(K)	Ref.	Notes
28	2400–2700*	1	Ni,Co; *T fixed by peridotite liquidus; f_{O_2}≈ IW-0.5 (expt.)
27	2200	2	Ni,Co,P,Mo,W; f_{O_2} = IW-0.15 (inf.)
37	2300	3	Ni,Co,Fe; Cr requires 3400K
>35	>3600	4	V,Cr,Mn; f_{O_2} = IW-2.3 (inf.)
43–59	2400–4200	5	Ni,Co; f_{O_2} = IW to IW-2 (expt.)
25*	3350	6	Si; *P fixed by Ni/Co data; temp exceeds peridotite liquidus
27	2250	7	P,W,Co,Ni,Mo,Re,Ga,Sn,Cu; f_{O_2} = IW-0.4 (inf.)
40	2800	8	Ni,Co
40	3750*	9	V,Ni,Co,Mn,Si; *T fixed by peridotite liquidus; evolving f_{O_2}?
30–60	>2000	10	Ni,Co; f_{O_2} = IW-2.2 (inf.); demonstrates solution tradeoffs

f_{O_2} is the oxygen fugacity, IW indicates the iron–wustite buffer, 'inf.' means inferred f_{O_2} for the magma ocean and 'expt.' indicates the experimental value. 1, Li and Agee (1996); 2, Righter *et al.* (1997); 3, O'Neill *et al.*, (1998); 4, Gessmann and Rubie, (2000); 5, Li and Agee (2001); 6, Gessmann *et al.* (2001); 7, Righter and Drake (2003); 8, Walter and Trønnes (2004); 9, Wade and Wood (2005); 10, Chabot *et al.* (2005).

base of a magma ocean that deepens as the Earth grows in size. The temperature at the base of the magma ocean is constrained to lie on the peridotite liquidus. In order to satisfy the observed mantle abundances of all elements considered (and especially V), it is necessary that the oxygen fugacity is initially very low but increases during accretion to satisfy the current FeO content of the mantle (**Figure 15**). The explanation for the increase in f_{O_2} involves the crystallization of silicate perovskite from the magma ocean, which can only occur once the Earth has reached a critical size such that the pressure at the base of the magma ocean reaches ~24 GPa. Because of its crystal chemistry, the crystallization of silicate perovskite causes ferrous iron to dissociate to ferric iron + metallic iron by the reaction:

$$Fe^{2+} \rightarrow Fe^{3+} + Fe$$

silicate liquid perovskite metal

(Frost *et al.*, 2004). If some or all of the metal produced by this reaction is transferred from the mantle to the core, the Fe^{3+} content and the f_{O_2} of the mantle both increase. Although this model can explain the abundances of MSEs in the mantle, ~0.5% of chondritic material has to be added to the Earth at a late stage of accretion in order to generate the observed chondritic ratios of the HSEs (see Section 9.03.3.2.2.(ii)).

There is at least one potential problem with the model of Wade and Wood (2005). At very low oxygen fugacities (≤IW-3), Ta becomes siderophile and would therefore be extracted from the mantle during core formation (Mann *et al.*, 2006). However, the abundance of Ta in the mantle is chondritic which may exclude the possibility of the initially low oxygen fugacity conditions proposed by Wade and Wood (2005).

9.03.3.2.2.(ii) The 'late-veneer' hypothesis

According to this hypothesis, the main stage of core formation involved the almost complete extraction of HSEs from the mantle into the metallic core, under reducing oxygen-fugacity conditions (e.g., Kimura *et al.*, 1974; Morgan, 1986; O'Neill and Palme, 1998; Righter, 2005). At a late stage of accretion, a thin veneer of chondritic material was added to the Earth under relatively oxidizing conditions, such that the HSEs were retained in the mantle in approximately chondritic ratios. The mass of material added at this late stage is considered to be <1% of the entire mantle. This is currently the most widely accepted 'heterogeneous' core-formation model. However, the likelihood that Ta would be extracted into the core under reducing conditions (Mann *et al.*, 2006) is a problem, as discussed in the previous section, because the mantle has not been depleted in this element.

9.03.3.2.2.(iii) Inefficient core formation

Originally suggested by Jones and Drake (1986), this hypothesis proposes that a small quantity of metallic Fe was trapped in the mantle during core formation. The current HSE budget of the mantle was supplied by this stranded metal. One objection to this hypothesis is that Earth is likely to have been largely molten during core formation, with the result that metal segregation should have been very efficient (Righter, 2005). However, based on the study of Frost *et al.* (2004), it is likely that not all metal

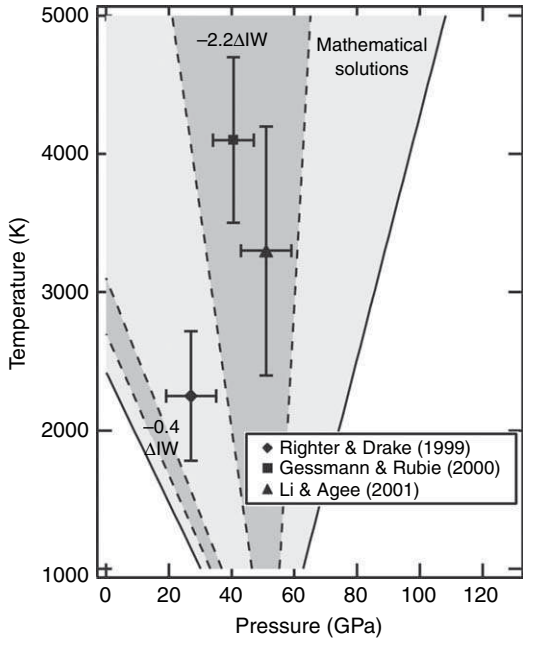

Figure 14 Pressure–temperature conditions of metal–silicate equilibration during core formation that are consistent with the concentrations of Ni and Co in the Earth's mantle, based on experimental studies of the metal–silicate partitioning of these elements. The two dark-gray shaded regions show results calculated for oxygen fugacities of IW-0.4 and IW-2.2, respectively, whereas the light-shaded region shows solutions for all oxygen fugacities. *P–T* estimates from three previous studies are shown by the symbols with error bars. Temperature is poorly constrained because the partition coefficients for Ni and Co depend only weakly on this variable. In order to better constrain the *P–T* conditions of equilibration, it is necessary to consider additional siderophile elements for which partitioning is more strongly temperature dependent (e.g., Wade and Wood, 2005). Reproduced from Chabot NL, Draper DS, and Agee CB (2005) Conditions of core formation in the Earth: Constraints from nickel and cobalt partitioning. *Geochemica et Cosmochemica Acta* 69: 2141–2151, with permission from Elsevier.

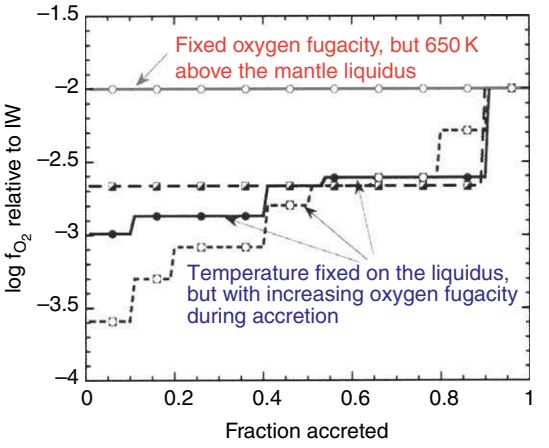

Figure 15 Models involving continuous core formation during accretion of the Earth based on metal–silicate equilibration at the base of a deepening magma ocean. Oxygen fugacity is plotted as a function of fraction accreted. The temperature at the base of the magma ocean is constrained to lie on the peridotite liquidus for the variable oxygen fugacity models. In order to satisfy concentrations of a range of siderophile elements in the mantle, the oxygen fugacity has to be low initially and then increase during accretion for reasons described in the text. Reprinted from Wood BJ, Walter MJ, and Wade J (2006) Accretion of the Earth and segregation of its core. *Nature* 441: 825–833 (doi:10.1038/nature04763), with permission of Macmillan Publishers Ltd.

segregated to the core during crystallization of the molten Earth. The argument runs as follows: As described above (Section 9.03.3.2.2.(i)), the crystallization of silicate perovskite, the dominant phase of the lower mantle, involved the disproportionation reaction $Fe^{2+} \rightarrow Fe^{3+} + Fe$ metal. The subsequent loss of some of this metal to the core resulted in an increase in the oxidation state of the mantle – which explains why the Earth's mantle has been oxidized during or after core formation (Frost *et al.*, 2004; Wood and Halliday, 2005; Wood *et al.*, 2006). However, if all the metal produced by perovskite crystallization had been extracted to the core, the mantle would now be much more oxidized than is observed. In the Martian mantle, there is, at most, only a thin lower mantle containing silicate perovskite. The paucity (or absence) of silicate perovskite thus explains, based on the observations of Frost *et al.* (2004), why the Martian mantle is more reduced than Earth's mantle (Wadhwa, 2001; Herd *et al.*, 2002). However, the possibility of a small fraction of metal being trapped during core formation on Mars still exists and could explain the similarities between HSE abundances in the mantles of Earth and Mars (thus making the more complex late-veneer hypothesis redundant). Recently, inefficient core formation has also been suggested to result from deformation-enhanced percolation (Hustoft and Kohlstedt, 2006), as discussed above in Section 9.03.2.3.1.

9.03.3.2.2.(iv) Addition of outer-core material to the lower mantle It has been suggested that HSE abundances in the Earth's mantle have resulted from core–mantle interaction (Brandon and Walker, 2005), for example, by the addition of a small amount of core metal to the mantle (Snow and Schmidt, 1998). This could potentially occur by capillary

action (considered highly unlikely by Poirier *et al.* (1998)) or by dilatancy caused by volume strain (Rushmer *et al.*, 2005; Kanda and Stevenson, 2006). Alternatively, siderophile elements could be added to the base of the mantle by crystallization of oxides or silicates due to the growth of the inner core (Walker, 2000, 2005) and chemical exchange could be facilitated by the (possible) presence of partial melt in the lower few kilometers of the mantle. In this case, the metal–silicate partition coefficients at CMB conditions would have to be orders of magnitude lower than at low P–T conditions and would need to result in the addition of the HSEs in approximately chondritic proportions.

9.03.3.2.3 Metal–silicate fractionation models

The simplest model of metal–silicate fractionation during core formation involves the ponding of liquid iron at the base of a convecting magma ocean with chemical equilibration occurring at the metal–silicate interface (Section 9.03.3.2.2.(i), **Figure 9(a)**). An appealing feature of this model is that siderophile element abundances in the mantle can be interpreted directly in terms of magma ocean depth (e.g., Li and Agee, 1996; Righter *et al.*, 1997). The timescale required for chemical equilibration across the metal–silicate interface has been investigated by Rubie *et al.* (2003) assuming that mass transport occurs by chemical diffusion across boundary layers that exist above and below the interface. As described earlier, a magma ocean is expected to crystallize from the bottom up which means that the initial crystallization of silicate minerals at the base of the magma ocean will terminate equilibration between the ponded iron and the overlying magma ocean. Thus, Rubie *et al.* (2003) also calculated the timescale required for the initial crystallization of the base of the magma ocean. Results are dependent upon the depth of the magma ocean and suggest that equilibration times are almost three orders of magnitude greater than cooling times (**Figure 16**). Such a result is also predicted by considering that rates of conductive heat transfer are much faster than rates of chemical diffusion (Rubie *et al.*, 2003). Therefore, these results appear to rule out simple chemical equilibration at the base of the magma ocean.

The equilibration model of Rubie *et al.* (2003) is based on the assumption that a dense atmosphere was not present during magma ocean crystallization. The effect of such an insulating atmosphere would be to reduce the rate of heat loss and therefore prolong the lifetime of the magma ocean. However, the rate of convection would also be reduced, which would slow the rate of chemical exchange across the metal–silicate interface. Thus, the presence of an insulating atmosphere is unlikely to affect the conclusions of Rubie *et al.* (2003). However, there has been a recent suggestion that a magma ocean adiabat is much steeper than formerly believed with the consequence that terrestrial magma oceans might crystallize from the top down rather than from the bottom up (Mosenfelder *et al.*, 2007; cf. Miller *et al.*, 1991). In this case, magma ocean crystallization would be much slower and the possibility of simple metal–silicate equilibration at its base might need to be reconsidered.

It is currently assumed in core-formation models that metal–silicate separation takes place in a magma ocean of global extent and of more or less constant depth (**Figure 9**). As discussed above in Section 9.03.2.3.2, this assumption requires reconsideration. **Figure 17** shows an alternative model in which the magma ocean that is generated by a large impact is initially a hemispherical body of limited lateral extent. The attainment of isostatic equilibrium eventually results in the formation of a global magma ocean but metal segregation could already have taken place before this developed. Pressure at the base of the initial hemispherical magma ocean is clearly much higher than at the base of the final global magma ocean, which means that the partitioning of siderophile elements could depend critically on the timing of metal segregation.

As discussed above, liquid metal is likely to be present in a magma ocean in the form of small droplets ~1 cm in diameter. Such droplets remain in chemical equilibration with the magma as the they settle out and P–T conditions change because diffusion distances are short (Karato and Murthy, 1997; Rubie *et al.*, 2003). It is necessary to understand the chemical consequences of the settling out of such droplets in order to interpret siderophile element geochemistry in terms of magma ocean depths. Rubie *et al.* (2003) considered two end-member models for the partitioning of Ni. The models are based on the parametrized Ni partitioning formulation of Righter and Drake (1999) which requires a magma ocean depth of ~800 km for metal–silicate equilibration at its base to produce the estimated core–mantle partition coefficient of ~28. In model 1 of Rubie *et al.* (2003), the magma ocean is static (i.e., no convection or mixing) and droplets that are initially uniformly dispersed settle out and re-equilibrate progressively as they

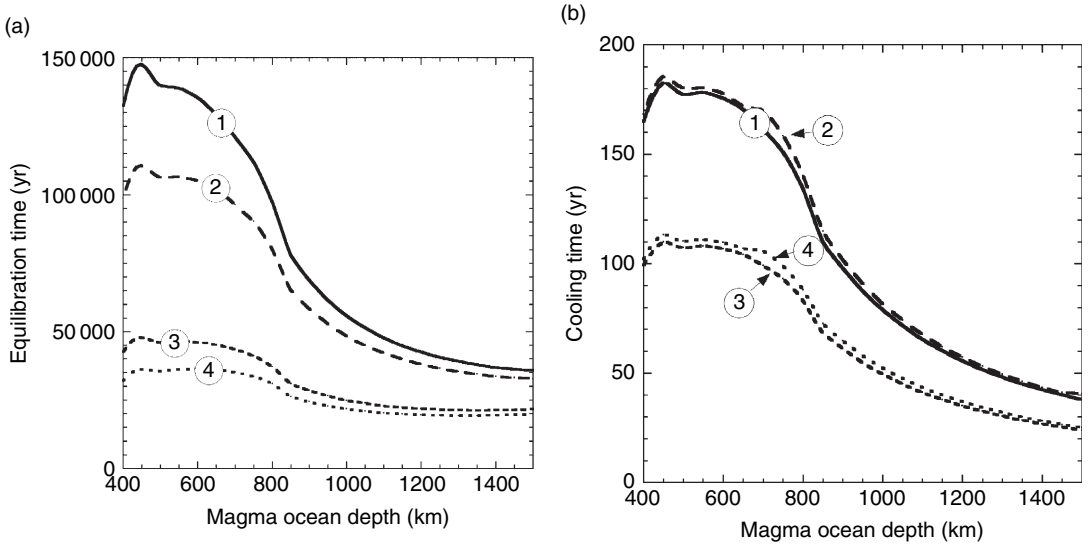

Figure 16 Results of a model in which a layer of segregated (ponded) liquid iron equilibrates chemically with an overlying convecting magma ocean. (a) Time to reach 99% equilibration between metal and silicate as a function of magma ocean depth. (b) Time required for initial crystallization at the base of the magma ocean (thus effectively terminating the equilibration process). The four curves (1–4) are results for a wide range of plausible model parameters. Reproduced from Rubie DC, Melosh HJ, Reid JE, Liebske C, and Righter K (2003) Mechanisms of metal-silicate equilibration in the terrestrial magma ocean. *Earth and Planetary Science Letters* 205: 239–255, with permission from Elsevier.

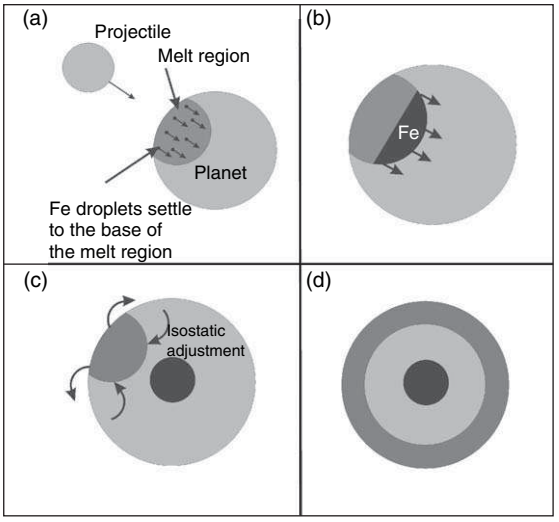

Figure 17 Possible evolution of a deep magma ocean that forms as a consequence of a giant impact. (a) Initially a hemispherical magma ocean forms that is of limited lateral extent. There is the possibility that iron, emulsified in the form of small dispersed droplets, settles and segregates rapidly to form a protocore at the bottom of this magma ocean (b and c). Subsequent isostatic adjustment causes the magma ocean to evolve into a layer of global extent (d). The relative timing of the processes of metal segregation and isostatic adjustment determines the pressure (and probably also temperature) conditions of metal–silicate equilibration. Reproduced from Tonks WB and Melosh HJ (1992) Core formation by giant impacts. *Icarus* 100: 326–346, with permission from Elsevier.

fall. This polybaric equilibration model requires a magma ocean ~1400 km deep (**Figure 18**) because much of the silicate equilibrates at relatively low pressures where $D_{Ni}^{met-sil}$ values are high. Model 2 of Rubie *et al.* (2003) is based on an assumption of vigorous convection keeping the magma ocean fully mixed and chemically homogeneous. The iron droplets equilibrate finally with silicate liquid at the base of the magma ocean just before segregating into a ponded layer. Because the mass fraction of metal that is available to equilibrate with silicate progressively decreases with time, the effectiveness of metal to remove siderophile elements from the magma ocean also decreases. This model requires a magma ocean ~550 km deep to produce the desired core–mantle partition coefficient of 28 (**Figure 18**).

The two end-member models 1 and 2 are clearly both physically unrealistic and a more realistic result must lie somewhere between the two extremes shown in **Figure 18**. In an attempt to investigate the chemical consequences of metal–silicate segregation in a deep magma ocean more rigorously, Höink *et al.* (2006) have combined two- and three-dimensional numerical convection models with a tracer-based sedimentation method. They found that metal droplets stabilize the magma ocean against convection and that convection only develops in the upper layer of a magma ocean after it has become depleted

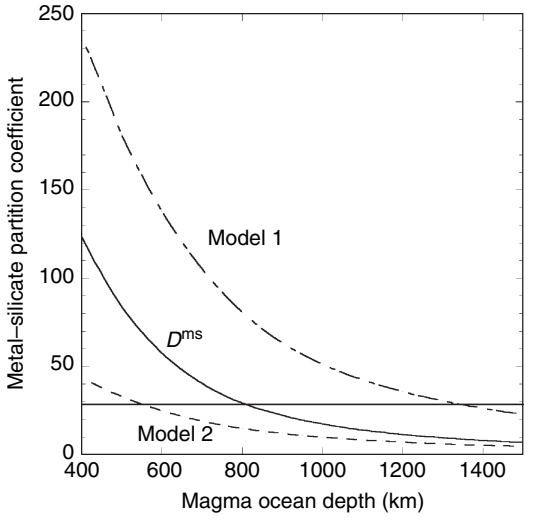

Figure 18 Results of different metal–silicate fractionation models for the siderophile element Ni as a function of magma ocean depth. The core–mantle partition coefficient for this element is estimated to be ~28 (as indicated by the horizontal line). The curve labeled D^{ms} indicates results for simple equilibration between a ponded liquid metal layer and the overlying magma ocean and requires a magma ocean ~800 km deep to obtain the core–mantle value. However, this model is unlikely to be realistic (**Figure 16**). Models 1 and 2 represent extreme end-member cases (see text for details) and require magma ocean depths of ~1400 and ~550 km, respectively. Reproduced from Rubie DC, Melosh HJ, Reid JE, Liebske C, and Righter K (2003) Mechanisms of metal-silicate equilibration in the terrestrial magma ocean. *Earth and Planetary Science Letters* 205: 239–255, with permission from Elsevier.

in iron droplets. The timescale for droplet separation was found to be identical to the Stokes' settling time. Because of the lack of convection in the droplet-dominated layer, the chemical consequences are similar to those of model 1 of Rubie *et al.* (2003), although the results of the two- and three-dimensional models of Höink *et al.* (2006) appear to be very different from each other (see their figure 20). An alternative approach has been adopted by Melosh and Rubie (2007) using a two-dimensional model for computing the flow of two interpenetrating fluids (liquid silicate and liquid iron). Their preliminary results also suggest that droplets settle out in approximately the Stokes' settling time but show that strong density currents develop in the droplet-bearing region of the magma ocean due to density perturbations. The velocities of these density currents range up to $50\,m\,s^{-1}$, which is much greater than velocities induced by thermal convection. In addition, the gravitational energy of sinking droplets is converted into heat which raises the temperature at the base of the magma ocean by at least several hundred degrees. Based on these preliminary results, it is not yet clear how the partitioning of siderophile elements compares with the predictions of the Höink *et al.* models. This is a rapidly developing area of research and controversy at the moment.

9.03.3.2.4 Concluding remarks

The consistency of MSE abundances with metal–silicate equilibration at high P,T conditions, implies that abundances produced by earlier equilibration in smaller bodies at lower P,T conditions must have been overprinted. This conclusion supports the idea of impactor cores undergoing re-equilibration in the magma ocean, presumably as a result of emulsification (Rubie *et al.*, 2003). Later events which did not involve re-equilibration (e.g., the descent of large iron diapirs through the lower mantle) would not leave any signature in the siderophile element abundances.

9.03.3.3 Light Elements in the Core

The density of the Earth's core is too low, by 5–10%, for it to consist only of Fe and Ni (e.g., Birch, 1952; Anderson and Isaak, 2002). It has therefore been postulated that the core must contain up to ~10 wt.% of one or more light elements, with the most likely candidates being S, O, Si, C, P, and H (Poirier, 1994). Knowledge of the identity of the light element(s) is important for constraining the bulk composition of the Earth, for understanding processes occurring at the CMB and how such processes are affected by crystallization of the inner core (e.g., Buffett *et al.* (2000); Helffrich and Kaneshima, 2004). The main constraints on the identity of the light elements present in the core are based on cosmochemical arguments (McDonough, 2003), experimental data (Hillgren *et al.*, 2000; Li and Fei, 2003), and computational simulations (e.g., Alfe *et al.*, 2002). The topic has been reviewed recently by Hillgren *et al.* (2000), McDonough (2003), and Li and Fei (2003) and here we provide only a brief summary of the main arguments and recent experimental results.

The sulfur content of the core, based on the relative volatility of this element, is likely to be no more than 1.5–2 wt.%, (McDonough and Sun, 1995; Dreibus and Palme, 1996; McDonough, 2003). Similarly, cosmochemical constraints suggest that only very small amounts (e.g., $\leq$0.2 wt.%) of C and P are present in the core (McDonough, 2003);

therefore these elements are unlikely to contribute significantly to the density deficit.

One of the main controversies concerning the identity of the principle light element(s) in the core involves silicon and oxygen. A high oxygen content is favored by high oxygen fugacity, whereas a high Si content is favored by low oxygen fugacity (Kilburn and Wood, 1997; Hillgren *et al.*, 2000; Li and Fei, 2003; Malavergne *et al.*, 2004). It has therefore been proposed that these two elements are almost mutually exclusive (**Figure 19**; O' Neill *et al.*, 1998). Some models of core composition have been based on this exclusivity; that is, it is assumed that the core contains either Si or O but not both of these elements (McDonough, 2003; table 7). However, the effects of high pressure and temperature are also critical.

Based on experimental results of Gessmann *et al.* (2001), obtained up to 23 GPa and 2473 K, the solubility of Si in liquid iron increases with both P and T. An extrapolation of their experimental data shows that ~7 wt.% Si can be dissolved in liquid Fe at 25–30 GPa, 3100–3300 K, and an f_{O_2} (IW-2) that is expected for core formation (**Figure 20(a)**). This result is in accordance with the geochemical model of the core of Allegre *et al.* (1995) in which ~7 wt.% Si in the core was proposed based on the Mg/Si ratio of the mantle being high compared with CI chondrites. However, according to thermodynamic arguments of Gessmann *et al.* (2001), the solubility

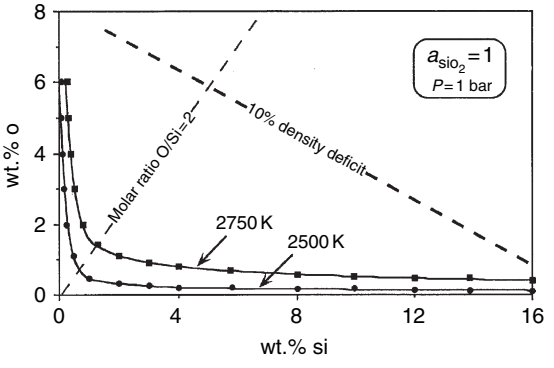

Figure 19 Mutual solubilities of O and Si in liquid iron at 1 bar. Because high O concentrations are favored by high f_{O_2} and high Si solubilities require a low f_{O_2}, the solubilities of these elements are mutually exclusive. The dashed line indicates solubilities required to account for the 10% density deficit of the core. Reproduced from O'Neill HSC, Canil D, and Rubie DC (1998) Oxide-metal equilibria to 2500°C and 25 GPa: Implications for core formation and the light component in the Earth's core. *Journal of Geophysical Research* 103: 12239–12260, with permission of American geophysical Union.

of Si in liquid Fe is predicted to decrease with pressure above ~30 GPa in the mantle and to approach zero at conditions of the CMB (**Figure 20(b)**). The reason for the postulated reversal in pressure dependence is that the coordination of Si^{4+} in mantle silicates changes from fourfold to sixfold at ~25 GPa which reverses the sign of the volume change (ΔV) of the exchange reaction of Si between silicates and liquid Fe.

Oxygen was first proposed as the principal light element in the core about 30 years ago (e.g., Ringwood, 1977; Ohtani and Ringwood, 1984; Ohtani *et al.*, 1984). Although it is clear that the solubility of this element in liquid Fe increases with temperature, the effect of pressure has been controversial. According to studies of phase relations in the Fe–FeO system, solubility increases with pressure (Ringwood, 1977; Kato and Ringwood, 1989). However, investigations of the partitioning of FeO between magnesiowüstite and liquid Fe have indicated that solubility decreases with increasing pressure and, based on a very large extrapolation, is essentially zero at conditions of the CMB (O'Neill *et al.*, 1998; Rubie *et al.*, 2004). Asahara *et al.* (2007) may have resolved the controversy by showing that the partitioning of FeO into liquid Fe decreases weakly with pressure up to ~15 GPa and then increases again at high pressures. The reason for the change in pressure dependence is that the FeO component dissolved in liquid Fe is more compressible than FeO dissolved in an oxide or silicate phase. Thus, the sign of the volume change (ΔV) of the exchange reaction of oxygen between silicates/oxides and liquid Fe reverses at 10–15 GPa (see also Ohtani *et al.*, 1984; Walker, 2005). As discussed below, the partitioning of oxygen into liquid iron appears to be high enough at core-formation conditions for this element to be the most abundant light element in the Earth's core (Rubie *et al.*, 2004; Asahara *et al.*, 2007).

Recent studies using the LH-DAC suggest that concentrations of both oxygen and silicon could be significant in the core and could, in combination, account for the density deficit. Takafuji *et al.* (2005) found 3 wt.% Si and 5 wt.% O in liquid Fe in equilibrium with $(Mg,Fe)SiO_3$ perovskite at 97 GPa and 3150 K. In similar experiments on liquid Fe coexisting with the post-perovskite phase, Sakai *et al.* (2006) found up to 6.3 wt.% O and 4 wt.% Si in liquid Fe at 139 GPa and 3000 K. These results should be regarded as preliminary because of the huge temperature gradients and large temperature uncertainties that are characteristic of LH-DAC experiments; in addition,

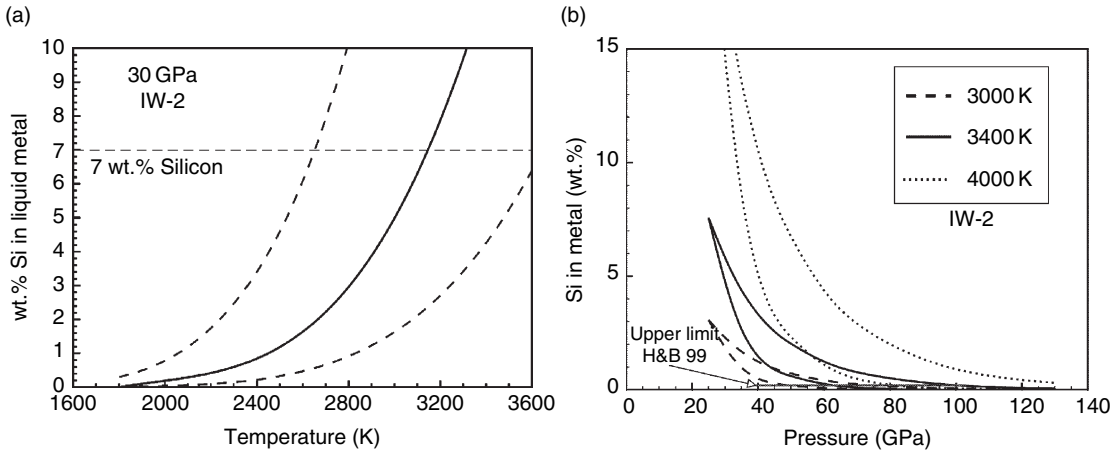

Figure 20 (a) Solubility of Si in liquid Fe alloy at 30 GPa and an oxygen fugacity of IW-2 based on an extrapolation of experimental data. The dashed lines show the extent of the uncertainty envelope based on error propagation. (b) Extrapolation of the experimental data to core conditions at an oxygen fugacity of IW-2. Here the pressure dependence is predicted to be opposite to that at low pressures due to Si being incorporated in silicates in six-fold coordination at pressures above 25–30 GPa; this structural change causes the volume change of the exchange reaction of Si between metal and silicate to reverse. Also shown are diamond anvil cell results (H&B99) of Hillgren and Boehler (1999) that were obtained at 45–100 GPa and an unknown oxygen fugacity. Reproduced from Gessmann CK, Wood BJ, Rubie DC, and Kilburn MR (2001) Solubility of silicon in liquid metal at high pressure: Implications for the composition of the Earth's core. *Earth Planetary Science Letters* 184: 367–376, with permission from Elsevier.

the oxygen fugacity was probably not buffered. In the case of oxygen, the LH-DAC results are mostly consistent with the lower pressure data of Asahara *et al.* (2007). However, the silicon results indicate considerably higher solubilities than those predicted by Gessmann *et al.* (2001) which may indicate that the volume change of the exchange reaction of Si between silicates and Fe metal assumed in the latter study is too large. The high mutual solubilities of O and Si, compared with low P–T results (O'Neill *et al.*, 1998), could be largely the consequence of high temperatures.

An additional important observation is that the outer core has a larger density deficit and therefore appears to contain a higher concentration of light element(s) than the inner core (Jephcoat and Olson, 1987; Alfe *et al.*, 2002). This implies that the light element(s) partitions strongly into liquid iron during freezing, which is potentially diagnostic behavior. For instance, Alfe *et al.* (2002), using molecular dynamics simulations, found that oxygen, due to its small atomic radius, tends to be expelled during the freezing of liquid iron. Conversely, S and Si have atomic radii similar to that of iron at core pressures, and thus substitute freely for iron in the solid inner core. Based on the observed density difference between the inner and outer cores, Alfe *et al.* (2002) predicted ~8 wt.% oxygen in the outer core. These results support the case for O being the main light element and are in agreement with the predictions of Asahara *et al.* (2007). Such molecular dynamics calculations have not yet been performed for either H or C, which might also behave in a similar manner to O.

The Earth's core is considered not to be in chemical equilibrium with the mantle (Stevenson, 1981) and light-element solubilities at core conditions are therefore not necessarily indicative of the actual concentrations of these elements in the core. Instead, the light-element content of the core is likely to have been set during core formation, as was the case for the siderophile elements. As discussed above, studies of the metal–silicate partitioning of the MSEs indicate that core–mantle partitioning is consistent with metal–silicate equilibration at conditions of 30–60 GPa and $\leq$4000 K (**Table 3**). Thus metal–silicate partitioning of light elements (e.g., O and Si) at such conditions may have determined the light-element content of the core. Rubie *et al.* (2004) investigated this possibility by modeling the partitioning of oxygen (actually the FeO component) between a silicate magma ocean and liquid Fe alloy during core formation as a function of magma ocean depth. Because oxygen solubility in liquid Fe increases strongly with temperature, FeO partitions increasingly into the Fe alloy as the magma ocean depth is increased beyond 1000 km,

leaving the silicate depleted in FeO (**Figure 21(a)**). The results of this model are consistent with equilibration in a magma ocean 1200–2000 km deep and with the Earth's core containing 7–8 wt.% oxygen.

The Earth's mantle contains ~8 wt.% FeO, whereas, based on studies of Martian meteorites, the Martian mantle is considered to contain ~18 wt.% FeO. This difference can be explained by oxygen partitioning during core formation so that the possibility that the two planets have similar (or even identical) bulk compositions cannot be excluded (Rubie *et al.*, 2004). Because Mars is a much smaller planet than Earth, temperatures and pressures in a Martian magma ocean are expected to have been relatively low, so that little FeO was extracted from the mantle during core formation (**Figure 21(b)**). This model also explains why the mass fraction of the Martian core is smaller than that of the Earth's core.

One advantage of modeling the metal–silicate partitioning of oxygen during core formation, in addition to the siderophile elements, is that assumptions concerning oxygen fugacity are not required. This is because the partitioning of oxygen determines the oxygen fugacity. Instead it is necessary to estimate the bulk composition (i.e., oxygen content) of the metal–silicate system, for example, on the basis of the chemistry of chondritic meteorites (Rubie *et al.*, 2004).

9.03.4 Summary

Theoretical arguments and geochemical observations suggest that the bulk of the mass of the Earth accreted through a few, large impacts within about 50 My of solar system formation, and that each of these impacts generated a global, if transient, magma ocean. Although the impacting bodies were undoubtedly differentiated, pre-existing chemical signals appear to have been overprinted by the impact process. Siderophile element concentrations are consistent with magma oceans extending at least to mid-mantle depths (800–1500 km, 2500–4000 K). The impactor cores likely underwent emulsification

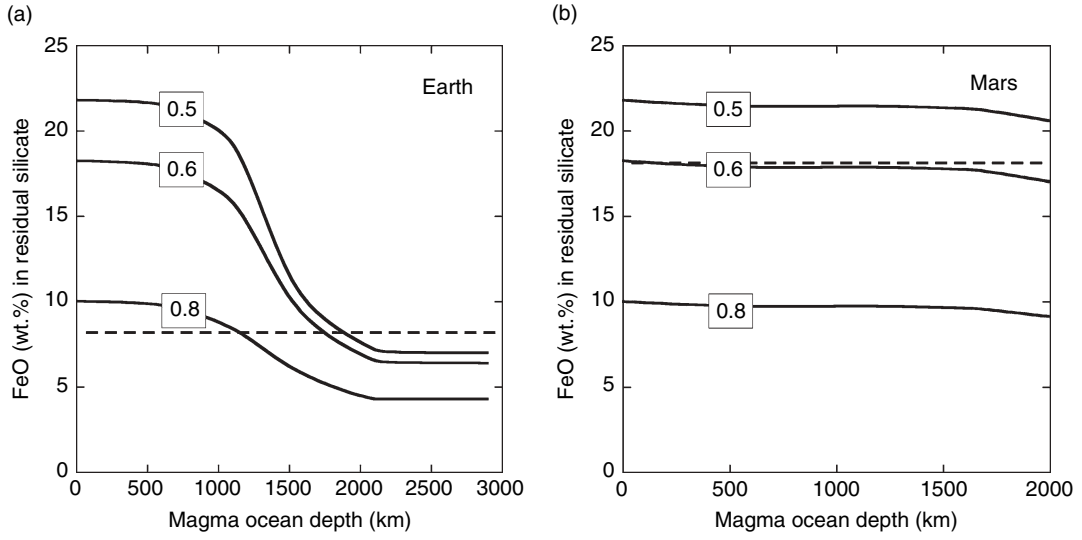

Figure 21 Results of core-formation models for Earth (a) and Mars (b), based on metal–silicate partitioning of FeO in a magma ocean. The models are based on a chondritic bulk composition that consists initially of a mixture of metal and silicate components. The bulk oxygen content determines the fraction of metal that is present. The three curves, in each case, show results for different initial bulk oxygen contents and the labels indicate the weight fraction of Fe that is initially present as metal. The horizontal dashed lines show the current FeO contents of the respective mantles. On Earth, the FeO content of the residual silicate decreases when the magma ocean depth exceeds 1000 km, because, at high temperatures, FeO partitions into the metal phase. On Mars, such an effect is almost absent because magma ocean temperatures are relatively low because of the small size of the planet. These results show that the bulk compositions of Earth and Mars could be similar (e.g., curve labeled '0.6') and that the current FeO content of the Earth's mantle resulted from core formation in a magma ocean ~1800 km deep: in this case, the Earth's core could contain 7–8 wt.% oxygen. Reprinted from Rubie DC, Gessmann CK, and, Frost DJ (2004) Partitioning of oxygen during core formation on the Earth and Mars. *Nature* 429: 58–61, with permission from Macmillan Publishers Ltd.

as they sank through the magma ocean, resulting in a chemical re-equilibration that is also suggested by both siderophile and Hf–W isotopic observations. This re-equilibration ceased as the metal pooled at the base of the magma ocean; subsequent transport of the resulting large-scale iron masses to the growing core was rapid and will have resulted in a significant increase in core temperatures. Following the Moon-forming impact, the initial core temperature was probably at least 6000 K, suggesting that extensive melting occurred in the lowermost mantle.

Unusually, there is broad agreement between the geochemical constraints and geophysical expectations of the core's early history. Nonetheless, several important outstanding questions remain:

1. The physics of exactly what happens during giant impacts is poorly understood (Sections 9.03.2.2.2 and 9.03.2.3.2). In particular, although there are physical and geochemical arguments for impactor emulsification, this process has not yet been investigated by numerical or laboratory models.
2. The lifetime of magma oceans is also poorly known (Section 9.03.2.3.2). This is in part because complicating factors such as the possible presence of an insulating atmosphere or a foundering crust have a large effect on the outcome. It may be that this is an issue which can only be resolved using radiogenic isotopes with appropriate half-lives, rather than geophysical modeling. In addition there is a possibility that terrestrial magma oceans may crystallize from the top down rather than from the bottom up (Mosenfelder *et al.*, 2007) – which could have major implications by greatly extending magma ocean lifetimes.
3. Geochemical models of core formation are currently hampered by a lack of partitioning data, especially for the HSEs at high pressures and temperatures. Even partitioning of MSEs is poorly known at pressures significantly above 25 GPa. Rectifying the latter deficiency requires laser-heated diamond anvil cell experiments (e.g., Tschauner *et al.*, 1999; Bouhifd and Jephcoat, 2003), which are difficult to perform successfully because of large temperature gradients (that can drive chemical diffusion), temperature uncertainties, and difficulties in sample analysis. An additional problem is that models of chemical fractionation during metal–silicate separation are not yet fully developed (Rubie *et al.*, 2003; Höink *et al.*, 2006, Melosh and Rubie, 2007).
4. Uncertainties remain concerning the identity of the light element(s) in the core. Based on cosmochemical arguments and recent high-pressure studies, oxygen may be the main light element together with ~2 wt.% S and a small amount of Si (see also Badro *et al.* 2007).
5. Most of the models of accretion and core formation to date have assumed single-stage processes. In practice, of course, accretion and core formation occurs as a series of discrete events, under evolving conditions. The effect of these changing conditions on the behavior and chemistry of the core and mantle is just beginning to be addressed (e.g., Halliday, 2004; Wade and Wood, 2005; Wood *et al.*, 2006). Unfortunately, although parameters like f_{O_2} likely evolved with time, all observations (except those of unstable isotopes) constrain only some time-weighted mean value of the parameter. Thus, resolving the time evolution of parameters such as f_{O_2} will be challenging and it may be difficult to identify unique solutions.

Acknowledgments

Portions of this work were supported by NSF-EAR, NASA-Origins, the German Science Foundation Priority Programme 'Mars and the Terrestrial Planets' (Grant Ru437) and an Alexander von Humboldt Senior Research Award to HJM.

References

Abe Y (1997) Thermal and chemical evolution of the terrestrial magma ocean. *Physics of the Earth and Planetary Interiors* 100: 27–39.

Agnor C and Asphaug E (2004) Accretion efficiency during planetary collisions. *Astrophysical Journal* 613: L157–L160.

Agnor CB, Canup RM, and Levison HF (1999) On the character and consequences of large impacts in the late stage of terrestrial planet formation. *Icarus* 142: 219–237.

Alfe D, Gillan MJ, and Price GD (2002) Composition and temperature of the Earth's core constrained by combining *ab initio* calculations and seismic data. *Earth and Planetary Science Letters* 195: 91–98.

Allegre CJ, Poirier J-P, Humler E, and Hofmann AW (1995) The chemical composition of the Earth. *Earth and Planetary Science Letters* 134: 515–526.

Anders E and Grevesse N (1989) Abundances of the elements: Meteoritic and solar. *Geochemica et Cosmochemica Acta* 53: 197–214.

Anderson OL and Isaak DG (2002) Another look at the core density deficit of Earth's outer core. *Physics of the Earth and Planetary Interiors* 131: 19–27.

Asahara Y, Frost DJ, and Rubie DC (2007) Partitioning of FeO between magnesiowüstite and liquid iron at high pressures and temperatures: Implications for the composition of the

Earth's outer core. *Earth and Planetary Science Letters* doi: 10.1016/j.epsl.2007.03.006.
Asphaug E, Agnor CB, and Williams Q (2006) Hit-and-run planetary collisions. *Nature* 439: 155–160.
Badro J, Fiquet G, Guyot F, *et al.* (2007) Effect of light elements on the sound velocities in solid iron: Implications for the composition of Earth's core. *Earth and Planetary Science Letters* 254: 233–238.
Baker J, Bizzarro M, Wittig N, Connelly J, and Haack H (2005) Early planetesimal melting from an age of 4.5662 Gyr for differentiated meteorites. *Nature* 436: 1127–1131.
Ballhaus C and Ellis DJ (1996) Mobility of core melts during Earth's accretion. *Earth and Planetary Science Letters* 143: 137–145.
Benz W and Cameron AGW (1990) Terrestrial effects of the giant impact. In: Newsom HE and Jones JH (eds.) *Origin of the Earth*, pp. 61–67. New York: Oxford University Press.
Benz W, Slattery WL, and Cameron AGW (1988) Collisional stripping of Mercury's mantle. *Icarus* 74: 516–528.
Birch F (1952) Elasticity and constitution of the Earth's interior. *Journal of Geophysical Research* 69: 227–286.
Blichert-Toft J, Gleason JD, Télouk P, and Albarède F (1999) The Lu–Hf isotope geochemistry of shergottites and the evolution of the Martian mantle–crust system. *Earth and Planetary Science Letters* 173: 25–39.
Boehler R (2000) High-pressure experiments and the phase diagram of lower mantle and core materials. *Reviews of Geophysics* 38: 221–245.
Borg LE and Draper DS (2003) A petrogenetic model for the origin and compositional variation of the martian basaltic meteorites. *Meteoritics and Planetary Science* 38: 1713–1731.
Bouhifd MA and Jephcoat AP (2003) The effect of pressure on the partitioning of Ni and Co between silicate and iron-rich metal liquids: A diamond-anvil cell study. *Earth and Planetary Science Letters* 209: 245–255.
Boyet M and Carlson RW (2005) Nd-142 evidence for early (> 4.53 Ga) global differentiation of the silicate Earth. *Science* 309: 576–581.
Brandon AD and Walker RJ (2005) The debate over core–mantle interaction. *Earth and Planetary Science Letters* 232: 211–225.
Bruhn D, Groebner N, and Kohlstedt DL (2000) An interconnected network of core-forming melts produced by shear deformation. *Nature* 403: 883–886.
Buffett BA, Garnero EJ, and Jeanloz R (2000) Sediments at the top of Earth's core. *Science* 290: 1338–1342.
Busso M, Gallino R, and Wasserburg GJ (1999) Nucleosynthesis in asymptotic giant branch stars: Relevance for galactic enrichment and solar system formation. *Annual Reviews of Astronomy and Astrophysics* 37: 239–309.
Cameron AGW (2000) High-resolution simulations of the giant impact. In: Canup RM and Righter K (eds.) *Origin of the Earth and Moon*, pp. 133–144. Tucson, AZ: University of Arizona Press.
Canup RM (2004) Simulations of a late lunar-forming impact. *Icarus* 168: 433–456.
Canup RM and Asphaug E (2001) Origin of the Moon in a giant impact near the end of the Earth's formation. *Nature* 412: 708–712.
Canup RM and Righter K (eds.) (2000) *Origin of the Earth and Moon*. Tucson, AZ: University of Arizona Press.
Canup RM, Ward WR, and Cameron AGW (2001) A scaling relationship for satellite-forming impacts. *Icarus* 150: 288–296.
Caro G, Bourdon B, Wood BJ, and Corgne A (2005) Trace-element fractionation in Hadean mantle generated by melt segregation from a magma ocean. *Nature* 436: 246–249.
Chabot NL and Agee CB (2003) Core formation in the Earth and Moon: New experimental constraints from V, Cr, and Mn. *Geochemica et Cosmochemica Acta* 67: 2077–2091.
Chabot NL, Draper DS, and Agee CB (2005) Conditions of core formation in the Earth: Constraints from Nickel and Cobalt partitioning. *Geochemica et Cosmochemica Acta* 69: 2141–2151.
Chabot NL and Haack H (2006) Evolution of asteroidal cores. In: Lauretta DS and McSween HY (eds.) *Meteorites and the Early Solar System*, pp. 747–771. Tucson, AZ: University of Arizona Press.
Chamberlin TC (1916) *The Origin of the Earth*, 271p. Chicago: University of Chicago Press.
Chambers JE (2003) Planet formation. In: Davis AM (ed.) *Treatise on Geochemistry, Vol. 1: Meteorites, Planets and Comets*, pp. 461–475. Oxford: Elsevier-Pergamon.
Chambers JE and Wetherill GW (1998) Making the terrestrial planets: N-body integrations of planetary embryos in three dimensions. *Icarus* 136: 304–327.
Clayton RN and Mayeda TK (1996) Oxygen isotope studies of achondrites. *Geochemica et Cosmochemica Acta* 60: 1999–2017.
Cottrell E and Walker D (2006) Constraints on core formation from Pt partitioning in mafic silicate liquids at high temperatures. *Geochemica et Cosmochemica Acta* 70: 1565–1580.
Dalziel SB, Linden PF, and Youngs DL (1999) Self-similarity and internal structure of turbulence induced by Rayleigh–Taylor instability. *Journal of Fluid Mechanics* 399: 1–48.
Drake MJ (2001) The eucrite/Vesta story. *Meteoritics and Planetary Science* 36: 501–513.
Drake MJ and Righter K (2002) Determining the composition of the Earth. *Nature* 416: 39–44.
Dreibus G and Palme H (1996) Cosmochemical constraints on the sulfur content in the Earth's core. *Geochemica et Cosmochemica Acta* 60: 1125–1130.
Elkins-Tanton LT, Parmentier EM, and Hess PC (2003) Magma ocean fractional crystallization and cumulate overturn in terrestrial planets: Implications for Mars. *Meteoritics and Planetary Science* 38: 1753–1771.
Elsasser WM (1963) Early history of the earth. In: Geiss J and Goldberg ED (eds.) *Earth Science and Meteoritics*, pp. 1–30. Amsterdam: North-Holland.
Ertel W, O'Neill HSC, Sylvester PJ, and Dingwell DB (1999) Solubilities of Pt and Rh in a haplobasaltic silicate melt at 1300°C. *Geochemica et Cosmochemica Acta* 63: 2439–2449.
Ertel W, O'Neill HSC, Sylvester PJ, Dingwell DB, and Spettel B (2001) The solubility of rhenium in silicate melts. Implications for the geochemical properties of rhenium at high temperatures. *Geochemica et Cosmochemica Acta* 65: 2161–2170.
Ertel W, Walter MJ, Drake MJ, and Sylvester PJ (2006) Experimental study of platinum solubility in silicate melt to 14 GPa and 2273 K: Implications for accretion and core formation in the Earth. *Geochemica et Cosmochemica Acta* 70: 2591–2602.
Faul UH (1997) Permeability of partially molten upper mantle rocks from experiments and percolation theory. *Journal of Geophysical Research* 102: 10299–10312 (doi:10.1029/96JB03460).
Fortenfant SS, Dingwell DB, Ertel-Ingrisch W, Capmas F, Birck JL, and Dalpé C (2006) Oxygen fugacity dependence of Os solubility in haplobasaltic melt. *Geochemica et Cosmochemica Acta* 70: 742–756.

Fortenfant SS, Günther D, Dingwell DB, and Rubie DC (2003a) Temperature dependence of Pt and Rh solubilities in a haplobasaltic melt. *Geochemica et Cosmochemica Acta* 67: 123–131.

Fortenfant SS, Rubie DC, Reid J, Dalpé C, and Gessmann CK (2003b) Partitioning of Re and Os between liquid metal and magnesiowüstite at high pressure. *Physics of the Earth and Planetary Interiors* 139: 77–91.

Frost DJ, Liebske C, Langenhorst F, McCammon CA, Trønnes RG, and Rubie DC (2004) Experimental evidence for the existence of iron-rich metal in the Earth′s lower mantle. *Nature* 428: 409–412.

Gaetani GA and Grove TL (1999) Wetting of mantle olivine by sulfide melt: Implications for Re/Os ratios in mantle peridotite and late-stage core formation. *Earth and Planetary Science Letters* 169: 147–163.

Gancarz AJ and Wasserburg GJ (1977) Initial Pb of the Amîtsoq gneiss, west Greenland, and implications for the age of the Earth. *Geochemica et Cosmochemica Acta* 41(9): 1283–1301.

Gessmann CK and Rubie DC (1998) The effect of temperature on the partitioning of Ni, Co, Mn, Cr and V at 9 GPa and constraints on formation of the Earth's core. *Geochemica et Cosmochemica Acta* 62: 867–882.

Gessmann CK and Rubie DC (2000) The origin of the depletions of V, Cr and Mn in the mantles of the Earth and Moon. *Earth and Planetary Science Letters* 184: 95–107.

Gessmann CK, Wood BJ, Rubie DC, and Kilburn MR (2001) Solubility of silicon in liquid metal at high pressure: Implications for the composition of the Earth′s core. *Earth and Planetary Science Letters* 184: 367–376.

Ghosh A and McSween HY (1998) A thermal model for the differentiation of Asteroid 4 Vesta, based on radiogenic heating. *Icarus* 134: 187–206.

Greenwood RC, Franchi IA, Jambon A, and Buchanan PC (2005) Widespread magma oceans on asteroid bodies in the early solar system. *Nature* 435: 916–918 (doi:10.1038/nature03612).

Grimm RE and McSween HY (1993) Heliocentric zoning of the asteroid belt by aluminum-26 heating. *Science* 259: 653–655.

Groebner N and Kohlstedt DL (2006) Deformation-induced metal melt networks in silicates: Implications for core–mantle interactions in planetary bodies. *Earth and Planetary Science Letters* 245: 571–580.

Haisch KE, Lada EA, and Lada CJ (2001) Disk frequencies and lifetimes in young clusters. *Astronomical Journal* 553: L153–L156.

Halliday AN (2003) The origin and earliest history of the Earth. In: Holland HD and Turekian KK (eds.) *Treatise on Geochemistry*, vol. 1, pp. 509–557. Amsterdam: Elsevier.

Halliday AN (2004) Mixing, volatile loss and compositional change during impact-driven accretion of the Earth. *Nature* 427: 505–509.

Hallworth MA, Phillips JC, Hubbert HE, and Sparks RSJ (1993) Entrainment in turbulent gravity currents. *Nature* 362: 829–831.

Hanks TC and Anderson DL (1969) The early thermal history of the Earth. *Physics of the Earth and Planetary Interiors* 2: 19–29.

Harper CL and Jacobsen SB (1996) Evidence for Hf-182 in the early solar system and constraints on the timescale of terrestrial accretion and core formation. *Geochemica et Cosmochemica Acta* 60: 1131–1153.

Helffrich G and Kaneshima S (2004) Seismological constraints on core composition from Fe-O-S liquid immiscibility. *Science* 306: 2239–2242.

Herd CDK, Borg LE, Jones JH, and Papike JJ (2002) Oxygen fugacity and geochemical variations in the martian basalts: Implications for Martian basalt petrogenesis and the oxidation state of the upper mantle of Mars. *Geochemica et Cosmochemica Acta* 66: 2025–2036.

Hillgren VJ, Drake MJ, and Rubie DC (1994) High-pressure and high-temperature experiments on core-mantle segregation in the accreting Earth. *Science* 264: 1442–1445.

Hillgren VJ, Gessmann CK, and Li J (2000) An experimental perspective on the light element in Earth′s core. In: Canup RM and Righter K (eds.) *Origin of the Earth and Moon*, pp. 245–264. Tucson, AZ: University of Arizona Press.

Höink T, Schmalzl J, and Hansen U (2006) Dynamics of metal-silicate separation in a terrestrial magma ocean. *Geochemistry Geophysics Geosystems* 7: Q09008 (doi:10.1029/2006GC001268).

Holzheid A, Schmitz MD, and Grove TL (2000a) Textural equilibria of iron sulphide liquids in partly molten silicate aggregates and their relevance to core formation scenarios. *Journal of Geophysical Research* 105: 13555–13567.

Holzheid A, Sylvester P, O'Neill HSC, Rubie DC, and Palme H (2000b) Evidence for a late chondritic veneer in the Earth's mantle from high-pressure partitioning of palladium and platinum. *Nature* 406: 396–399.

Hustoft JW and Kohlstedt DL (2006) Metal-silicate segregation in deforming dunitic rocks. *Geochemistry Geophysics Geosystems* 7: Q02001 (doi:10.1029/2005GC001048).

Iida T and Guthrie RL (1988) *The Physical Properties of Liquid Metals*, pp. 109–146. Oxford: Clarendon.

Jacobsen SB (2005) The Hf-W isotopic system and the origin of the Earth and Moon. *Annual Review of Earth and Planetary Sciences* 33: 531–570.

Jeffreys H (1952) *The Earth, 3rd edn. Cambridge: Cambridge University Press.*

Jephcoat A and Olson P (1987) Is the inner core of the Earth pure iron? *Nature* 325: 332–335.

Jones JH, Capobianco CJ, and Drake MJ (1992) Siderophile elements and the Earth's formation. *Science* 257: 1281–1282.

Jones JH and Drake MJ (1986) Geochemical constraints on core formation in the Earth. *Nature* 322: 221–228.

Jones JH, Neal CR, and Ely JC (2003) Signatures of the siderophile elements in the SNC meteorites and Mars: A review and petrologic synthesis. *Chemical Geology* 196: 21–41.

Kanda R and Stevenson DJ (2006) Suction mechanism for iron entrainment into the lower mantle. *Geophysical Research Letters* 33: L02310 (doi:10.1029/2005GL025009).

Karato SI and Murthy VR (1997) Core formation and chemical equilibrium in the Earth. Part I: Physical considerations. *Physics of the Earth and Planetary Interiors* 100: 61–79.

Kato T and Ringwood AE (1989) Melting relationships in the system Fe–FeO at high pressure: Implications for the composition and formation of the Earth's core. *Physics and Chemistry of Minerals* 16: 524–538.

Kaula WM (1979) Thermal evolution of the Earth and Moon growing by planetesimal impacts. *Journal of Geophysical Research* 84: 999–1008.

Kegler P, Holzheid A, Rubie DC, Frost DJ, and Palme H (2005) New results of metal/silicate partitioning of Ni and Co at elevated pressures and temperatures. *XXXVI Lunar and Planetary Science Conference*, Abstract #2030.

Keil K, Stoeffler D, Love SG, and Scott ERD (1997) Constraints on the role of impact heating and melting in asteroids. *Meteoritics and Planetary Science* 32: 349–363.

Keppler H and Rubie DC (1993) Pressure-induced coordination changes of transition-metal ions in silicate melts. *Nature* 364: 54–55.

Kilburn MR and Wood BJ (1997) Metal-silicate partitioning and the incompatibility of S and Si during core formation. *Earth and Planetary Science Letters* 152: 139–148.

Kimura K, Lewis RS, and Anders E (1974) Distribution of gold between nickel–iron and silicate melts: Implications for the abundances of siderophile elements on the Earth and Moon. *Geochemica et Cosmochemica Acta* 38: 683–701.

Kleine T, Palme H, Mezger M, and Halliday AN (2005) Hf-W chronometry of lunar metals and the age and early differentiation of the Moon. *Science* 310: 1671–1673.

Kleine T, Munker C, Mezger K, and Palme H (2002) Rapid accretion and early core formation on asteroids and the terrestrial planets from Hf–W chronometry. *Nature* 418: 952–955.

Kokubo E and Ida S (1998) Oligarchic growth of protoplanets. *Icarus* 131: 171–178.

Kominami J, Tanaka H, and Ida S (2005) Orbital evolution and accretion of protoplanets tidally interacting with a gas disk. Part I: Effects of interaction with planetesimals and other protoplanets. *Icarus* 178: 540–552.

Kong P, Ebihara M, and Palme H (1999) Siderophile elements in Martian meteorites and implications for core formation in Mars. *Geochemica et Cosmochemica Acta* 63: 1865–1875.

Kyte FT (1998) A meteorite from the Cretaceous/Tertiary boundary. *Nature* 396: 237–239.

Laporte D and Watson EB (1995) Experimental and theoretical constraints on melt distribution in crustal sources: The effect of crystalline anisotropy on melt interconnectivity. *Chemical Geology* 124: 161–184.

Li J and Agee CB (1996) Geochemistry of mantle–core differentiation at high pressure. *Nature* 381: 686–689.

Li J and Agee CB (2001) The effect of pressure, temperature, oxygen fugacity and composition on partitioning of nickel and cobalt between liquid Fe–Ni–S alloy and liquid silicate: Implications for the Earth′s core formation. *Geochemica et Cosmochemica Acta* 65: 1821–1832.

Li J and Fei Y (2003) Experimental constraints on core composition. In: Holland HD and Turekian KK (eds.) *Treatise on Geochemistry, vol. 2: The Mantle and Core*, pp. 521–546. Oxford: Elsevier-Pergamon.

Liebske C, Schmickler B, Terasaki H, *et al.* (2005) Viscosity of peridotite liquid up to 13 GPa: Implications for magma ocean viscosities. *Earth and Planetary Science Letters* 240: 589–604.

Lindstrom DJ and Jones JH (1996) Neutron activation analysis of multiple 10–100 μg glass samples from siderophile element partitioning experiments. *Geochemica et Cosmochemica Acta* 60: 1195–1203.

Lodders K and Fegley B (1998) *The Planetary Scientist's Companion*. New York: Oxford University Press.

Maier WD, Andreoli MAG, McDonald I, *et al.* (2006) Discovery of a 25-cm asteroid clast in the giant Morokweng impact crater, South Africa. *Nature* 441: 203–206.

Malavergne V, Siebert J, Guyot F, *et al.* (2004) Si in the core? New high-pressure and high-temperature experimental data. *Geochimica et Cosmochemica Acta* 68: 4201–4211.

Mann U, Frost DJ, Rubie DC, Shearer CK, and Agee CB (2006) Is silicon a light element in Earth's core? – Constraints from liquid metal – liquid silicate partitioning of some lithophile elements. *XXXVII Lunar and Planetary Science Conference*, Abstract #1161.

Matsui T and Abe Y (1986) Impact-induced atmospheres and oceans on Earth and Venus. *Nature* 322: 526–528.

McDonough WF (2003) Compositional model for the Earth′s core. In: Holland HD and Turekian KK (eds.) *Treatise on Geochemistry*, pp. 517–568. Oxford: Elsevier.

McDonough WF and Sun S-s (1995) The composition of the Earth. *Chemical Geology* 120: 223–253.

McSween HY (1999) *Meteorites and Their Parent Planets*. Cambridge, UK: Cambridge University Press.

Melosh HJ (1990) Giant impacts and the thermal state of the early Earth. In: Newsom NE and Jones JE (eds.) *Origin of the Earth*, pp. 69–83. Oxford: Oxford University Press.

Melosh HJ and Rubie DC (2007) Ni partitioning in the terrestrial magma ocean: A polybaric numerical model. *Lunar and Planetary Science XXXVIII* Abstract #1593.

Miller GH, Stolper EM, and Ahrens TJ (1991) The equation of state of a molten komatiite. Part 2: Application to komatiite petrogenesis and the Hadean mantle. *Journal of Geophysical Research* 96: 11849–11864.

Minarik WG, Ryerson FJ, and Watson EB (1996) Textural entrapment of core-forming melts. *Science* 272: 530–533.

Morbidelli A, Chambers J, Lunine JI, *et al.* (2000) Source regions and timescales for the delivery of water to the Earth. *Meteoritics and Planetary Science* 35: 1309–1320.

Morgan JW (1986) Ultramafic xenoliths: Clues to Earth's late accretionary history. *Journal of Geophysical Research* 91: 12375–12387.

Mosenfelder JL, Asimow PD, and Ahrens TJ (2007) Thermodynamic properties of Mg_2SiO_4 liquid at ultra-high pressures from shock measurements to 200 GPa on forsterite and wadsleyite. *Journal of Geophysical Research* (in press).

Murthy VR (1991) Early differentiation of the Earth and the problem of mantle siderophile elements – A new approach. *Science* 253: 303–306.

Nimmo F and Agnor CB (2006) Isotopic outcomes of N-body accretion simulations: Constraints on equilibration processes during large impacts from Hf-W observations. *Earth and Planetary Science Letters* 243: 26–43.

Ohtani E and Ringwood AE (1984) Composition of the core. Part I: Solubility of oxygen in molten iron at high temperatures. *Earth and Planetary Science Letters* 71: 85–93.

Ohtani E, Ringwood AE, and Hibberson W (1984) Composition of the core. Part II: Effect of high pressure on solubility of FeO in molten iron. *Earth and Planetary Science Letters* 71: 94–103.

Ohtani E and Yurimoto H (1996) Element partitioning between metallic liquid, magnesiowüstite, and silicate liquid at 20 GPa and 2500°C: A secondary ion mass spectrometric study. *Geophysical Research Letters* 23: 1993–1996.

O'Neill HSC (1992) Siderophile elements and the Earth's formation. *Science* 257: 1282–1284.

O'Neill HSC, Canil D, and Rubie DC (1998) Oxide-metal equilibria to 2500°C and 25 GPa: Implications for core formation and the light component in the Earth's core. *Journal of Geophysical Research* 103: 12239–12260.

O'Neill HSC and Palme H (1998) Composition of the silicate Earth: Implications for accretion and core formation. In: Jackson I (ed.) *The Earth's Mantle*, pp. 3–126. Cambridge, UK: Cambridge University Press.

Newsom HE (1990) Accretion and core formation in the Earth: Evidence from siderophile elements. In: Newsom HE and Jones JH (eds.) *Origin of the Earth*, pp. 273–288. New York: Oxford University Press.

Palme H and O'Neill HSC (2003) Cosmochemical estimates of mantle composition. In: Holland HD and Turekian KK (eds.) *Treatise on Geochemistry, vol. 2: The Mantle and Core*, pp. 1–38. Oxford: Elsevier-Pergamon.

Palme H, O'Neill H, St. C, and Benz W (2003) Evidence for collisional erosion of the Earth. *XXXIV Lunar and Planetary Science Conference*, Abstract #1741.

Pierazzo E, Vickery AM, and Melosh HJ (1997) A re-evaluation of impact melt production. *Icarus* 127: 408–432.

Poirier JP (1994) Light elements in the Earth's outer core: A critical review. *Physics of the Earth and Planetary Interiors* 85: 319–337.

Poirier JP, Malavergne V, and Le Mouël JL (1998) Is there a thin electrically conducting layer at the base of the mantle? In: Gurnis M, Wysession ME, Knittle E, and Buffett BA (eds.) *Geodynamics 28: The Core–Mantle Boundary Region*, pp. 131–137. Washington, DC: American Geophysical Union.

Porcelli D, Woolum D, and Cassen P (2001) Deep Earth rare gases: Initial inventories, capture from the solar nebula, and losses during Moon formation. *Earth and Planetary Science Letters* 193: 237–251.

Pritchard ME and Stevenson DJ (2000) Thermal aspects of a lunar origin by giant impact. In: Canum RM and Righter K (eds.) *Origin of the Earth and Moon*, pp. 179–196. Tucson, AZ: University of Arizona Press.

Quitté G, Latkoczy C, Halliday AN, Schönbächler M, and Günther D (2005) Iron-60 in the Eucrite parent body and the initial $^{60}Fe/^{56}Fe$ of the solar system. *LPSC XXXVI*, Abstract 1827.

Ranen MC and Jacobsen SB (2006) Barium isotopes in chondritic meteorites: Implications for planetary reservoir models. *Science* 314: 809–812.

Raymond SN, Quinn T, and Lunine JI (2004) Making other Earths: Dynamical simulations of terrestrial planet formation and water delivery. *Icarus* 168: 1–17.

Reid JE, Suzuki A, Funakoshi K, *et al.* (2003) The viscosity of $CaMgSi_2O_6$ liquid at pressures up to 13 GPa. *Physics of the Earth and Planetary Interiors* 139: 45–54.

Righter K (2003) Metal-silicate partitioning of siderophile elements and core formation in the early Earth. *Annual Review of Earth and Planetary Sciences* 31: 135–174.

Righter K (2005) Highly siderophile elements: Constraints on Earth accretion and early differentiation. In: van der Hilst RD, Bass JD, Matas J, and Trampert J (eds.) *Geophysical Monograph 160: Earth's Deep Mantle: Structure, Composition and Evolution*, pp. 201–218. Washington, DC: American Geophysical Union.

Righter K and Drake MJ (1996) Core Formation in Earth's Moon, Mars, and Vesta. *Icarus* 124: 513–529.

Righter K and Drake MJ (1997) Metal-silicate equilibrium in a homogeneously accreting Earth: New results for Re. *Earth and Planetary Science Letters* 146: 541–553.

Righter K and Drake MJ (1999) Effect of water on metal-silicate partitioning of siderophile elements: A high pressure and temperature terrestrial magma ocean and core formation. *Earth and Planetary Science Letters* 171: 383–399.

Righter K and Drake MJ (2000) Metal-silicate equilibration in the early Earth: New constraints from volatile moderately siderophile elements Ga, Sn, Cu and P. *Geochemica et Cosmochemica Acta* 64: 3581–3597.

Righter K and Drake MJ (2001) Constraints on the depth of an early terrestrial magma ocean. *Meteoritics and Planetary Science* 36: A173.

Righter K and Drake MJ (2003) Partition coefficients at high pressure and temperature. In: Carlson RW (ed.) *Treatise on Geochemistry*, vol. 2, pp. 425–449. Oxford: Elsevier.

Righter K, Drake MJ, and Yaxley G (1997) Prediction of siderophile element metal-silicate partition coefficients to 20 GPa and 2800 degrees C: The effects of pressure, temperature, oxygen fugacity, and silicate and metallic melt compositions. *Physics of the Earth and Planetary Interiors* 100: 115–134.

Ringwood AE (1977) Composition of the core and implications for the origin of the Earth. *Geochemical Journal* 11: 111–135.

Rose LA and Brenan JM (2001) Wetting properties of Fe–Ni–Co–Cu–O–S melts against olivine: Implications for sulfide melt mobility. *Economic Geology and Bulletin of the Society of Economics Geologists* 96: 145–157.

Rubie DC, Gessmann CK, and Frost DJ (2004) Partitioning of oxygen during core formation on the Earth and Mars. *Nature* 429: 58–61.

Rubie DC, Melosh HJ, Reid JE, Liebske C, and Righter K (2003) Mechanisms of metal-silicate equilibration in the terrestrial magma ocean. *Earth and Planetary Science Letters* 205: 239–255.

Rubin AM (1995) Propagation of magma-filled cracks. *Annual Review of Earth and Planetary Sciences* 23: 287–336.

Rushmer T, Minarik WG, and Taylor GJ (2000) Physical processes of core formation. In: Canup RM and Righter K (eds.) *Origin of the Earth and Moon*, pp. 227–244. Tucson, AZ: University of Arizona Press.

Rushmer T, Petford N, Humayun M, and Campbell AJ (2005) Fe-liquid segregation in deforming planetesimals: Coupling core-forming compositions with transport phenomena. *Earth and Planetary Science Letters* 239: 185–202.

Russell CT and Luhmann JG (1997) Mercury: Magnetic field and magnetosphere. In: Shirley JH and Fairbridge RW (eds.) *Encyclopedia of Planetary Sciences*, pp. 476–478. New York: Chapman and Hall.

Ruzicka A, Snyder GA, and Taylor LA (1997) Vesta as the howardite, eucrite and diogenite parent body: Implications for the size of a core and for large-scale differentiation. *Meteoritics and Planetary Science* 32: 825–840.

Safronov VS (1978) The heating of the Earth during its formation. *Icarus* 33: 1–12.

Sakai T, Kanto T, Ohtani E, *et al.* (2006) Interaction between iron and post-perovskite at core–mantle boundary and core signature in plume source region. *Geophysical Research Letters* 33: L15317 (doi 10.1029/2006GL026868).

Scherstén A, Elliott T, Hawkesworth C, Russell S, and Massarik J (2006) Hf-W evidence for rapid differentiation of iron meteorite parent bodies. *Earth and Planetary Science Letters* 241: 530–542.

Schmickler B, Liebske C, Holzapfel C, and Rubie DC (2005) Viscosity of peridotite liquid up to 24 GPa: Predictions from self-diffusion coefficients. *EOS Transactions American Geophysical Union* 86(52): Fall Meeting Supplement, Abstract MR11A-06.

Schoenberg R, Kamber BS, Collerson KD, and Eugster O (2002) New W-isotope evidence for rapid terrestrial accretion and very early core formation. *Geochemica et Cosmochemica Acta* 66: 3151–3160.

Schramm DN, Tera F, and Wasserburg GJ (1970) The isotopic abundance of ^{26}Mg and limits on ^{26}Al in the early solar system. *Earth and Planetary Science Letters* 10: 44–59.

Schubert G, Anderson JD, Spohn T, and McKinnon WB (2004) Interior composition, structure and dynamics of the Galilean satellites. In: Bagenal F, Dowling T, and Mckinnon WB (eds.) *Jupiter: The Planet, Satellites and Magnetosphere*, pp. 281–306. Cambridge, UK: Cambridge University Press.

Shannon MC and Agee CB (1996) High pressure constraints on percolative core formation. *Geophysical Research Letters* 23: 2717–2720.

Shannon MC and Agee CB (1998) Percolation of core melts at lower mantle conditions. *Science* 280: 1059–1061.

Snow JE and Schmidt G (1998) Constraints on Earth accretion deduced from noble metals in the oceanic mantle. *Nature* 391: 166–169.

Solomatov VS (2000) Fluid dynamics of a terrestrial magma ocean. In: Canup RM and Righter K (eds.) *Origin of the Earth and Moon*, pp. 323–338. Tucson, AZ: University of Arizona Press.

Solomon S (1979) Formation, history and energetics of cores in the terrestrial planets. *Physics of the Earth and Planetary Interiors* 19: 168–182.

Spohn T and Schubert G (1991) Thermal equilibration of the Earth following a giant impact. *Geophysical Journal International* 107: 163–170.

Stevenson DJ (1981) Models of the Earth's core. *Science* 214: 611–619.

Stevenson DJ (1989) Formation and early evolution of the Earth. In: Peltier WR (ed.) *Mantle Convection plate tectonics and global dynamics*, pp. 817–873. New York: Gordon and Breach.

Stevenson DJ (1990) Fluid dynamics of core formation. In: Newsom HE and Jones JH (eds.) *Origin of the Earth*, pp. 231–250. New York: Oxford University Press.

Stevenson DJ (2003) Mission to the Earth's core – A modest proposal. *Nature* 423: 239–240.

Tachibana S, Huss GR, Kita NT, Shimoda G, and Morishita Y (2006) Fe-60 in chondrites: Debris from a nearby supernova in the early solar system? *Astrophysical Journal* 639: L87–L90.

Taylor SR and Norman MD (1990) Accretion of differentiated planetesimals to the Earth. In: Newsom HE and Jones JH (eds.) *Origin of the Earth*, pp. 29–43. New York: Oxford University Press.

Takafuji N, Hirose K, Mitome M, and Bando Y (2005) Solubilities of O and Si in liquid iron in equilibrium with (Mg,Fe), SiO_3 perovskite and the light elements in the core. *Geophysical Research Letters* 32: L06313 (doi: 10.1029/2005GLO22773).

Takafuji N, Hirose K, Ono S, Xu F, Mitome M, and Bando Y (2004) Segregation of core melts by permeable flow in the lower mantle. *Earth and Planetary Science Letters* 224: 249–257.

Terasaki H, Frost DJ, Rubie DC, and Langenhorst F (2005) The effect of oxygen and sulphur on the dihedral angle between Fe–O–S melt and silicate minerals at high pressure: Implications for Martian core formation. *Earth and Planetary Science Letters* 232: 379–392 (doi:10.1016/j.epsl.2005.01.030).

Terasaki H, Frost DJ, Rubie DC, and Langenhorst F (2007a) Percolative core formation in planetesimals. *Earth and Planetary Science Letters* (in press).

Terasaki H, Frost DJ, Rubie DC, and Langenhorst F (2007b) The interconnectivity of Fe–O–S liquid in polycrystalline silicate perovskite at lower mantle conditions. *Physics of the Earth and Planetary Interiors* (in press).

Thibault Y and Walter MJ (1995) The influence of pressure and temperature on the metal-silicate partition coefficients of nickel and cobalt in a model C1 chondrite and implications for metal segregation in a deep magma ocean. *Geochemica et Cosmochemica Acta* 59: 991–1002.

Thomas PC, Parker JW, McFadden LA, *et al.* (2005) Differentiation of the asteroid Ceres as revealed by its shape. *Nature* 437: 224–226.

Thomson W and Tait PG (1883) *Treatise on Natural Philosophy*, 527p. Cambridge: Cambridge University Press.

Tonks WB and Melosh HJ (1992) Core formation by giant impacts. *Icarus* 100: 326–346.

Tonks WB and Melosh HJ (1993) Magma ocean formation due to giant impacts. *Journal of Geophysical Research* 98: 5319–5333.

Treiman AH, Jones JH, and Drake MJ (1987) Core formation in the Shergottite parent body and comparison with the Earth. *Journal of Geophysical Research* 92: E627–E632.

Tschauner O, Zerr A, Specht S, Rocholl A, Boehler R, and Palme H (1999) Partitioning of nickel and cobalt between silicate perovskite and metal at pressures up to 80 GPa. *Nature* 398: 604–607 (doi:10.1038/19287).

Turan JW (1984) Nucleosynthesis. *Annual Review of Nuclear and Particle Science* 34: 53–97.

Turcotte DL and Schubert G (2002) *Geodynamics*. Cambridge, UK: Cambridge University Press.

Urey HC (1952) *The Planets: Their Origin and Development*, 245p. New Haven, CT: Yale University Press.

von Bargen N and Waff HS (1986) Permeabilities, interfacial areas and curvatures of partially molten systems: Results of numerical computations of equilibrium microstructures. *Journal of Geophysical Research* 91: 9261–9276.

Wade J and Wood BJ (2005) Core formation and the oxidation state of the Earth. *Earth and Planetary Science Letters* 236: 78–95.

Wadhwa M (2001) Redox state of Mars' upper mantle and crust from Eu anomalies in Shergottite pyroxenes. *Science* 291: 1527–1530.

Walker D (2000) Core participation in mantle geochemistry: Geochemical Society Ingerson Lecture. *Geochemica et Cosmochemica Acta* 64: 2897–2911.

Walker D (2005) Core–mantle chemical issues. *Canadean Mineralogist* 43: 1553–1564.

Walker D, Norby L, and Jones JH (1993) Superheating effects on metal-silicate partitioning of siderophile elements. *Science* 262: 1858–1861.

Walte NP, Becker JK, Bons PD, Rubie DC, and Frost DJ (2007) Liquid distribution and attainment of textural equilibrium in a partially-molten crystalline system with a high-dihedral-angle liquid phase. *Earth and Planetary Science Letters* (in press).

Walter MJ, Newsom HE, Ertel W, and Holzheid A (2000) Siderophile elements in the Earth and Moon: Metal/silicate partitioning and implications for core formation. In: Canup RM and Righter K (eds.) *Origin of the Earth and Moon*, pp. 265–290. Tucson, AZ: University of Arizona Press.

Walter MJ and Thibault Y (1995) Partitioning of tungsten and molybdenum between metallic liquid and silicate melt. *Science* 270: 1186–1189.

Walter MJ and Trønnes RG (2004) Early Earth differentiation. *Earth and Planetary Science Letters* 225: 253–269.

Warren PH (1985) The magma ocean concept and lunar evolution. *Annual Review of Earth and Planetary Sciences* 13: 201–240.

Warren PH (1993) A concise compilation of petrologic information on possible pristine nonmare Moon rocks. *American Mineralogist* 78: 360–376.

Warren PH, Kallemeyn GW, and Kyte FT (1999) Origin of planetary cores: Evidence from highly siderophile elements in Martian meteorities. *Geochemica et Cosmochemica Acta* 63: 2105–2122.

Wasson JT (1985) *Meteorites: Their Record of Early Solar-System History*, 267p. New York: W. H. Freeman.

Weidenschilling SJ, Spaute D, Davis DR, Marzari F, and Ohtsuki K (1997) Accretional evolution of a planetesimal swarm. Part 2: The terrestrial zone. *Icarus* 128: 429–455.

Wetherill GW (1985) Occurrence of giant impacts during the growth of the terrestrial planets. *Science* 228: 877–879.

Wetherill GW (1990) Formation of the Earth. *Annual Review of Earth and Planetary Sciences* 18: 205–256.

Wetherill GW and Stewart GR (1993) Formation of planetary embryos – Effects of fragmentation, low relative velocity, and independent variation of eccentricity and inclination. *Icarus* 106: 190–209.

Williams J-P and Nimmo F (2004) Thermal evolution of the Martian core: Implications for an early dynamo. *Geology* 32: 97–100.

Williams Q and Hemley RJ (2001) Hydrogen in the deep Earth. *Annual Review of Earth and Planetary Sciences* 29: 365–418.

Wood BJ and Halliday AN (2005) Cooling of the Earth and core formation after the giant impact. *Nature* 437: 1345–1348.

Wood BJ, Walter MJ, and Wade J (2006) Accretion of the Earth and segregation of its core. *Nature* 441: 825–833 (doi:10.1038/nature04763).

Yin QZ, Jacobsen SB, Yamashita K, Blichert-Toft J, Telouk P, and Albarede F (2002) A short timescale for terrestrial planet formation from Hf-W chronometry of meteorites. *Nature* 418: 949–952.

Yoder CF (1995) Astrometric and geodetic properties of Earth and the solar system. In: Ahrens TJ (ed.) *Global Earth Physics*, pp. 1–31. Washington, DC: American Geophysical Union.

Yoshino T, Price JD, Wark DA, and Watson EB (2006) Effect of faceting on pore geometry in texturally equilibrated rocks: Implications for low permeability at low porosity. *Contributions to Mineralogy and Petrology* 152: 169–186 (doi:10.1007/s00410-006-0099-y).

Yoshino T, Walter MJ, and Katsura T (2003) Core formation in planetesimals triggered by permeable flow. *Nature* 422: 154–157.

Young GA (1965) *The Physics of the Base Surge*. US White Oak, MD: Naval Ordnance Laboratory.